The Plant Cell, Vol. 30: 700–716, March 2018, www.plantcell.org © 2018 ASPB.

A Functional Study of AUXILIN-LIKE1 and 2, Two Putative Clathrin Uncoating Factors in Arabidopsis[OPEN]

Maciek Adamowski,[a] Madhumitha Narasimhan,[a] Urszula Kania,[a,b,c,1] Matouš Glanc,[a,d] Geert De Jaeger,[b,c] and Jiří Friml[a,2]

[a] IST Austria, 3400 Klosterneuburg, Austria
[b] Ghent University, Department of Plant Biotechnology and Bioinformatics, 9052 Ghent, Belgium
[c] VIB Center for Plant Systems Biology, 9052 Ghent, Belgium
[d] Department of Experimental Plant Biology, Faculty of Science, Charles University, 12844 Prague, Czech Republic

ORCID IDs: 0000-0002-8600-0671 (M.N.); 0000-0003-0619-7783 (M.G.); 0000-0001-6558-5669 (G.D.J.); 0000-0002-8302-7596 (J.F.)

Clathrin-mediated endocytosis (CME) is a cellular trafficking process in which cargoes and lipids are internalized from the plasma membrane into vesicles coated with clathrin and adaptor proteins. CME is essential for many developmental and physiological processes in plants, but its underlying mechanism is not well characterized compared with that in yeast and animal systems. Here, we searched for new factors involved in CME in *Arabidopsis thaliana* by performing tandem affinity purification of proteins that interact with clathrin light chain, a principal component of the clathrin coat. Among the confirmed interactors, we found two putative homologs of the clathrin-coat uncoating factor auxilin previously described in non-plant systems. Overexpression of AUXILIN-LIKE1 and AUXILIN-LIKE2 in Arabidopsis caused an arrest of seedling growth and development. This was concomitant with inhibited endocytosis due to blocking of clathrin recruitment after the initial step of adaptor protein binding to the plasma membrane. By contrast, *auxilin-like1/2* loss-of-function lines did not present endocytosis-related developmental or cellular phenotypes under normal growth conditions. This work contributes to the ongoing characterization of the endocytotic machinery in plants and provides a robust tool for conditionally and specifically interfering with CME in Arabidopsis.

INTRODUCTION

The endomembrane system provides a spatial organization for plant cell activities by compartmentalizing distinct biochemical processes. The endomembrane system compartments, including the plasma membrane (PM), endoplasmic reticulum, Golgi stacks, *trans*-Golgi network/early endosome, multivesicular body, and vacuole perform distinct, specialized functions. At the cell periphery, endocytosis internalizes PM-localized proteins, lipids, and extracellular material. The best-characterized endocytic mechanism in plants depends on the coat protein clathrin. More than 20 years ago, clathrin-coated pits and vesicles were observed in plant cells by electron microscopy and vesicles were purified from plant tissues (Tanchak et al., 1984; Mersey et al., 1985; Emons and Traas, 1986; Galway et al., 1993). With the advent of *Arabidopsis thaliana* as a model system and the availability of mutants and live imaging techniques in recent times, CME has been further investigated (Dhonukshe et al., 2007; Kitakura et al., 2011; Wang et al., 2013a; Konopka et al., 2008). Despite these advances, detailed descriptions of the events that comprise CME in plants are still often based on the more advanced studies of CME in animal and yeast systems (reviewed in McMahon and Boucrot, 2011).

In non-plant systems, the endocytic process is initiated by the adaptor protein complex AP-2, which acts by interacting with specific PM lipids and endocytotic cargoes and through clathrin recruitment. Proteins of the FCH domain only (FCHo) family were also proposed to be initiation factors (Henne et al., 2010). In plants, two candidates for initiation factors are the conserved AP-2 complex (Di Rubbo et al., 2013; Kim et al., 2013; Yamaoka et al., 2013; Bashline et al., 2013; Fan et al., 2013) and the recently identified TPLATE adaptor protein complex (Gadeyne et al., 2014; Zhang et al., 2015). A family of genes encoding monomeric adaptors of the AP180 N-Terminal Homology and Epsin N-Terminal Homology (ANTH/ENTH) type is present in plant genomes as well (reviewed in Zouhar and Sauer, 2014). Clathrin-coated pits grow via the recruitment, by adaptors, of clathrin triskelions. These three-legged units of the clathrin coat are each composed of three clathrin light chains and three clathrin heavy chains (CLCs and CHCs, respectively). Clathrin triskelions assemble into a regularly shaped lattice surrounding the forming lipid vesicle. The scission (separation) of a completed vesicle from the PM is mediated by dynamins, i.e., molecular scissors that mechanically constrict the neck between the clathrin-coated vesicle (CCV) and the PM. In non-plant systems, upon scission, the CCV recruits uncoating factors, which are the molecular chaperone Hsc70 and its cochaperones auxilin/cyclin G-associated kinase (GAK) (Gao et al., 1991; Ahle and Ungewickell, 1990; Ungewickell et al., 1995; Massol et al., 2006; Xing et al., 2010). The uncoating step releases the vesicle for its subsequent fusion with endosomal compartments and allows the CME machinery components to be recycled for further rounds of endocytosis. The CCV-uncoating process is virtually uncharacterized in plants, although an auxilin-like

[1] Current address: The Sainsbury Laboratory Cambridge University, Cambridge CB2 1NN, UK.
[2] Address correspondence to jiri.friml@ist.ac.at.
The author responsible for distribution of materials integral to the findings presented in this article in accordance with the policy described in the Instructions for Authors (www.plantcell.org) is: Jiří Friml (jiri.friml@ist.ac.at).

www.plantcell.org/cgi/doi/10.1105/tpc.17.00785

protein of Arabidopsis is thought to have an uncoating function (Lam et al., 2001).

So far, endocytosis has been manipulated in plants through the use of clathrin mutants and a dominant negative version of CHC (Kitakura et al., 2011; Dhonukshe et al., 2007), lines with down-regulated expression of the endocytic adaptors (Gadeyne et al., 2014, Di Rubbo et al., 2013; Kim et al., 2013; Bashline et al., 2013; Fan et al., 2013), and mutants defective in dynamins (Yoshinari et al., 2016; Collings et al., 2008) and early endosomal components (Tanaka et al., 2013). These and similar tools allowed characterization of roles of CME in processes such as plant immunity (reviewed in Ben Khaled et al., 2015), establishment of polar auxin transport through the polarized subcellular localization of PIN-FORMED (PIN) auxin transporters (reviewed in Adamowski and Friml, 2015; Łangowski et al., 2016), and brassinosteroid signaling (Irani et al., 2012; Di Rubbo et al., 2013).

Here, our aim was to search for new proteins involved in CME in plants. To this end, we screened for proteins that bind to CLC, a fundamental component of the clathrin coat, in Arabidopsis. Based on several confirmed interactors, this study focused on two putative homologs of the uncoating factor auxilin. We found that overexpression of AUXILIN-LIKE1 and AUXILIN-LIKE2 caused an arrest of growth and development and inhibition of endocytosis, likely by preventing clathrin recruitment to endocytic pits initiated by the adaptor proteins. In contrast, loss of AUXILIN-LIKE1/2 function did not visibly interfere with development, or endocytosis, under optimal growth conditions.

RESULTS

Identification of CLC1-Associated Proteins

To search for new proteins involved in CME, we employed tandem affinity purification coupled with mass spectrometry (TAP-MS; Van Leene et al., 2014) using CLATHRIN LIGHT CHAIN1 (CLC1) as bait. We first expressed C- and N-terminal CLC1-TAP tag fusions in Arabidopsis cell suspensions, which was followed by protein isolation, affinity purification, and identification of clathrin-bound proteins by mass spectrometry. Using this technique, we identified a small number of clathrin binding proteins with sequence features indicating possible endocytic functions (Figure 1A).

The first identified were two highly homologous proteins containing DNAJ domains at their C termini. As such, they bear limited similarity to auxilins and GAKs, which also contain C-terminal DNAJ domains that are needed for Hsc70 recruitment and activation leading to clathrin uncoating (Ungewickell et al., 1995). We named the putative auxilin homologs AUXILIN-LIKE1 (AT4G12780) and AUXILIN-LIKE2 (AT4G12770). These two proteins belong to a family of seven proteins in Arabidopsis with C-terminal DNAJ domains, which can all therefore be called auxilin-likes. AUXILIN-LIKE1 is identical to the auxilin-like protein identified previously as a putative uncoating factor in Arabidopsis (Lam et al., 2001).

Second, we found CAP1, a monomeric adaptor protein that, together with its closest homolog ECA4 (Song et al., 2012), was identified based on interactions with the TPLATE endocytic adaptor protein complex (Gadeyne et al., 2014). CAP1 and ECA4 are part of a family of ANTH/ENTH adaptors that may be involved in the generation of coated vesicles at various sites of the endomembrane system (Zouhar and Sauer, 2014)

Third, we found SH3P2, a protein consisting of a central BAR domain and a C-terminal SH3 domain, the first of which acts in membrane curvature generation, while the second functions in protein-protein interactions. In animals, proteins with a similar BAR-SH3 domain composition are called endophilins and have been shown to act in a clathrin-independent endocytic pathway (Boucrot et al., 2014; Renard et al., 2014). SH3P2 belongs to a family of three proteins in Arabidopsis, the other two being SH3P1 and SH3P3 (Lam et al., 2001). SH3P2 has been implicated in the autophagy pathway (Zhuang et al., 2013, 2015), cell plate formation (Ahn et al., 2017), as well as vacuolar trafficking of ubiquitinated cargoes (Kolb et al., 2015; Nagel et al., 2017). Apart from AUXILIN-LIKE1/2, CAP1, and SH3P2, our TAP approach also identified the thioesterase DHNAT2, a peroxisome-localized enzyme (Widhalm et al., 2012), but we did not follow up on this finding. Finally, and as expected, we also identified both CHC homologs of Arabidopsis as well as two of the three homologs of CLC.

To confirm the interactions of the two auxilin-likes, CAP1, and SH3P2 with clathrin, we used bimolecular fluorescence complementation (BiFC), also known as the split-GFP assay (Kerppola, 2009). In this approach, two proteins of interest are fused to two complementary fragments of the GFP molecule and transiently coexpressed in wild tobacco (*Nicotiana benthamiana*) leaves via *Agrobacterium tumefaciens* injection. The physical proximity, or a direct interaction, of the two assayed proteins results in reconstitution of the GFP molecule and fluorescence, which is captured by confocal laser scanning microscopy (CLSM). Using this method, we confirmed the interactions of AUXILIN-LIKE1, AUXILIN-LIKE2, CAP1, and SH3P2 with CLC1 (Figure 1B). As a negative control, we probed for interactions of all these proteins with PHOSPHATIDYLINOSITOL 4,5-BISPHOSPHATE KINASE1 (PIP5K1; Tejos et al., 2014; Ischebeck et al., 2013), a peripheral PM-localized protein, and found no reconstituted GFP fluorescence (Supplemental Figure 1A). We also tested for interactions between our CLC-interacting proteins and observed interactions of AUXILIN-LIKE1/2 with SH3P2 and CAP1, but no interaction between SH3P2 and CAP1 (Supplemental Figure 1B). A summary of all BiFC interactions is presented in Figure 1C. The localization of the interacting pairs in wild tobacco cells appeared to be cytosolic. However, this is expected for soluble proteins, and we think it may not be indicative of the real interaction site of these proteins, as it is likely that reconstitution of a GFP molecule in the BiFC assay binds the two partners into stable dimers that subsequently don't exhibit normal localization and activity. Finally, SH3P2 was recently shown to interact with CHC (Nagel et al., 2017), while AUXILIN-LIKE1 was reported to interact with clathrin and with SH3P1, an SH3P2 homolog (Lam et al., 2001). These additional observations clearly support our interaction data.

In conclusion, our TAP and split-GFP data demonstrate interactions between clathrin, AUXILIN-LIKE1/2, CAP1, and SH3P2, suggesting a common function of these proteins.

Subcellular Localization of Clathrin-Associated Proteins

Next, we addressed the subcellular localization of the newly identified clathrin interactors (Figure 2; Supplemental Figure 2).

A

AGI code	Protein name	Isolated with (no. exp.)	
		C-terminal tag	N-terminal tag
AT4G12780 / AT4G12770	AUXILIN-LIKE1/2	2	-
AT4G32285	CAP1	2	-
AT4G34660	SH3P2	1	-
AT5G48950	DHNAT2	2	2
AT3G08530	Clathrin Heavy Chain1	2	2
AT3G11130	Clathrin Heavy Chain2	2	2
AT2G20760	Clathrin Light Chain1	2	2
AT2G40060	Clathrin Light Chain2	2	-

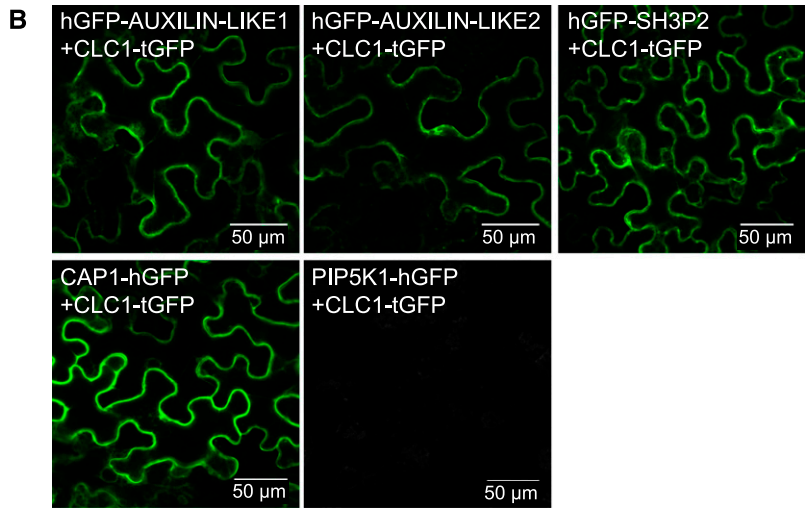

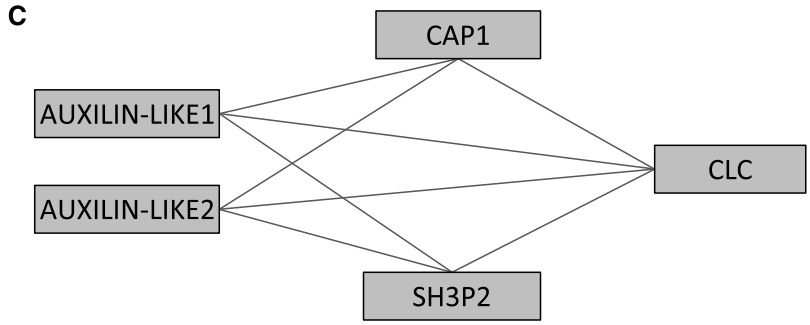

Figure 1. Identification of CLC-Interacting Proteins.

(A) TAP-MS-based isolation of proteins associated with clathrin. CLC1 in C- and N-terminal fusions with TAP tags was used as bait. Two repetitions with each construct were performed.

(B) BiFC-based interactions between CLC1 and selected interactors identified with TAP-MS. Pairs of proteins of interest fused with halves of the GFP molecule were transiently expressed in wild tobacco leaves and reconstituted GFP fluorescence was imaged in epidermis on the abaxial leaf side. PIP5K1 did not interact with any of the proteins tested and was used as a negative control.

(C) Schematic representation of all interactions detected with BiFC. Additional interactions are presented in Supplemental Figure 1.

We used CLSM on fluorescent protein fusions expressed in stable transgenic lines of Arabidopsis. We used a common model system for endomembrane trafficking studies, the epidermis of the seedling root apical meristem (RAM). To detect CAP1 localization, we cloned *CAP1*$_{pro}$*:CAP1-mCherry* and *35S*$_{pro}$*:CAP1-RFP* constructs and in both cases observed PM and cell plate binding (Figures 2A and 2B; Supplemental Figure 2A). Rarely, in ~10% of seedlings, CAP1 also showed binding to endosomal compartments (Supplemental Figure 2A). For SH3P2 localization, we used the previously published *UBQ*$_{pro}$*:SH3P2-GFP* line and cloned a *35S*$_{pro}$*:SH3P2-GFP* construct. Here too we observed PM and cell plate binding, as well as endosomal-like intracellular signals,

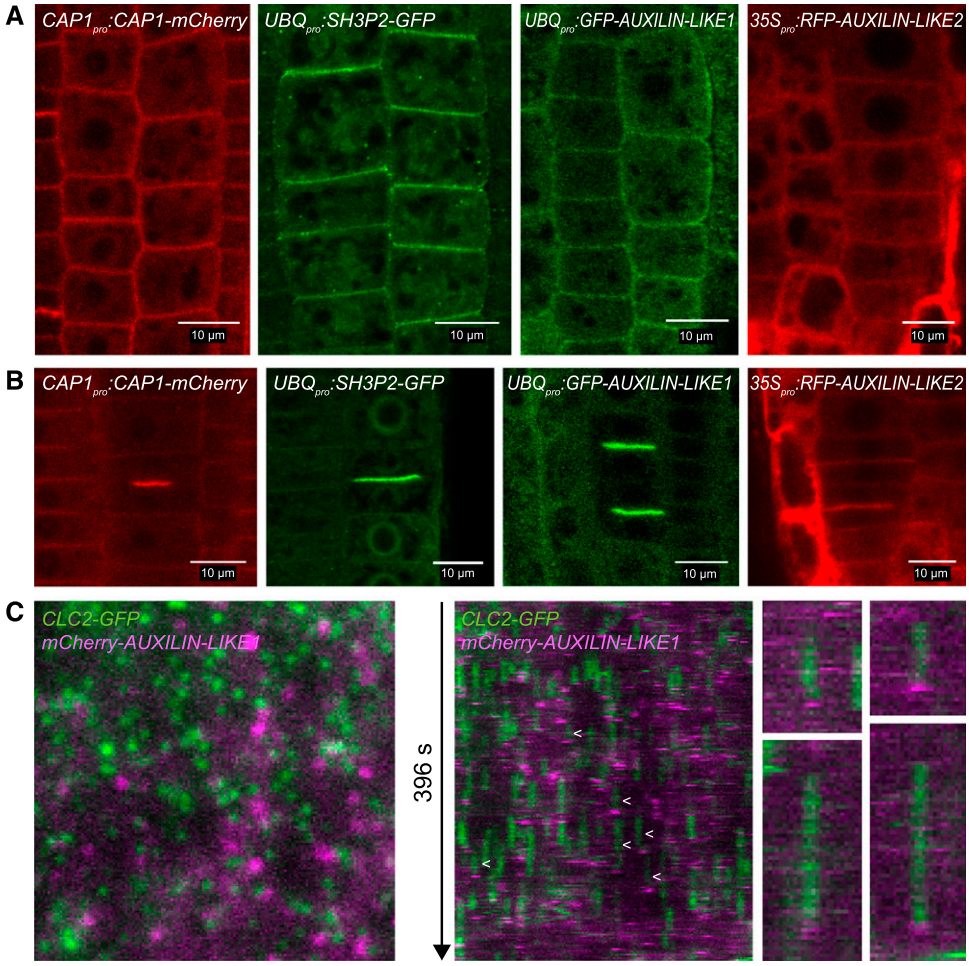

Figure 2. Subcellular Localizations of the Identified Clathrin Interactors.

(A) and **(B)** PM **(A)** and cell plate **(B)** localization of CAP1, SH3P2, AUXILIN-LIKE1, and AUXILIN-LIKE2 fluorescent protein fusions in the seedling root epidermis of stable transformants. Background cytosol staining can be observed in all lines, while CAP1 and SH3P2 also show faint nuclear staining. *35S$_{pro}$:RFP-AUXILIN-LIKE1* was identical to *35S$_{pro}$:RFP-AUXILIN-LIKE2*. Additional localization data, including colocalizations with PM markers, are presented in Supplemental Figure 2B.

(C) VAEM colocalization of clathrin (*CLC2$_{pro}$:CLC-GFP*) and AUXILIN-LIKE1 (*UBQ$_{pro}$:mCherry-AUXILIN-LIKE1*) in the hypocotyl epidermis. Kymographs (middle and right) show examples of auxilin-like1 recruitment at the end of CCP lifetime, which was observed in a small subset of all endocytic events (arrowheads). The majority of clathrin foci were lacking AUXILIN-LIKE1, and AUXILIN-LIKE1 foci without clathrin could be observed. See Supplemental Movie 1.

which were larger and more pronounced upon strong overexpression driven by the 35S promoter (Figures 2A and 2B; Supplemental Figure 2A). Our observations of SH3P2 localization are consistent with other recent reports (Ahn et al., 2017; Kolb et al., 2015; Nagel et al., 2017). We failed to clone the *AUXILIN-LIKE1/2* locus promoter region and instead prepared *UBQ10$_{pro}$:GFP-AUXILIN-LIKE1* as well as *35S$_{pro}$:RFP-AUXILIN-LIKE1* and *35S$_{pro}$:RFP-AUXILIN-LIKE2* constructs. Both auxilin-likes localized to the PM and cell plates, like CAP1 and SH3P2 (Figures 2A and 2B). Furthermore, all proteins of interest showed background cytosolic staining, while SH3P2 and CAP1 additionally weakly stained the nucleus. In summary, the localization patterns are consistent with a function of AUXILIN-LIKE1/2, CAP1, and SH3P2 in CME at the PM as well as clathrin-mediated processes at the cell plate. Additionally, SH3P2 functions at the endosomes, as has been demonstrated (Nagel et al., 2017), and the rarely observed endosomal localization of CAP1 suggests it may function there as well.

In animal cells, auxilins and GAKs are briefly recruited to clathrin-coated pits (CCPs) at the end of their lifetimes on the PM during the transition to vesicle budding (Massol et al., 2006; Lee et al., 2006). Apart from this late burst of auxilin recruitment, small and variable amounts of auxilin are present at earlier stages of CCP growth (Massol et al., 2006). Such events can be observed with total internal reflection fluorescence (TIRF) microscopy, a method that allows live imaging of the PM surface at high magnification. We wanted to address the recruitment of AUXILIN-LIKE1/2 to newly forming clathrin-coated vesicles in a similar manner. We

generated a double fluorescent reporter line, *CLC2$_{pro}$:CLC2-GFP* × *UBQ10$_{pro}$:mCherry-AUXILIN-LIKE1*, and employed variable angle epifluorescence microscopy (VAEM), a plant cell-specific TIRF-like method that allows the PM surface to be imaged through the plant cell walls, although it does not completely remove the cytoplasmic background below the PM (Konopka and Bednarek, 2008). In the epidermis of etiolated hypocotyls, AUXILIN-LIKE1 appeared as highly dynamic PM foci (Figure 2C; Supplemental Movie 1). With kymograph analysis, we observed events of brief AUXILIN-LIKE1 recruitment at the end of the lifetime of clathrin-coated pits, as previously described in non-plant systems. However, notably, we only observed this in a small fraction of all CCPs (estimated at around 5%), while the majority of clathrin-positive foci apparently did not recruit AUXILIN-LIKE1 (Figure 2C). We also regularly observed events of brief AUXILIN-LIKE1 recruitment at sites not containing clathrin. Based on these observations, we performed a control to assure that the observed colocalization events indeed represent specific late recruitment to coated pits. We looked at the kymographs for events where AUXILIN-LIKE1 signal appears not at the end, but around the beginning of a CLC2-GFP trace, which we consider to represent accidental colocalization. We found such events to be much more rare (16 versus 100 events in a single TIRF movie), which confirms that AUXILIN-LIKE1 is indeed specifically recruited at the end of the PM lifetime for at least a subpopulation of CCPs.

This observation might indicate that the majority of clathrin-coated vesicles do not use AUXILIN-LIKE1/2 for uncoating. Alternatively, perhaps AUXILIN-LIKE1/2 recruitment often takes place later after scission, when the vesicles had already moved away from the PM and thus had moved away from the variable region of VAEM detection. Some brief recruitment events could have also been missed because our method uses sequential scanning of the two fluorescent channels.

Seedling Phenotypes of AUXILIN-LIKE1/2 Overexpressors

While generating transgenic lines expressing fluorescent protein fusions of the clathrin-associated proteins, we observed that overexpressing *AUXILIN-LIKE1* and *AUXILIN-LIKE2* under the control of the 35S promoter was associated with deleterious phenotypes (Supplemental Figure 3B). In the T2 generation of *35S$_{pro}$:RFP-AUXILIN-LIKE1* and *35S$_{pro}$:RFP-AUXILIN-LIKE2* lines, we saw many seeds that did not germinate, even after prolonged culturing. Seeds that did germinate often developed slowly and exhibited relatively weak and patchy expression of RFP-AUXILIN-LIKE1/2 signals. In the T3 generation, a virtually complete silencing of the transgenes was observed. These observations reveal selection against high AUXILIN-LIKE1/2 expression levels, which was of interest to us, because overexpressing auxilins in non-plant systems can inhibit endocytosis (Zhao et al., 2001). In contrast, overexpression of CAP1 and SH3P2 in 35S-promoter-driven lines did not interfere with seed germination or seedling development (Supplemental Figure 3A). Therefore, we chose to follow up on the effects of AUXILIN-LIKE1/2 overexpression as a possible way to elucidate a clathrin-associated function of these two putative uncoating factors.

To circumvent the deleterious effects of constitutive AUXILIN-LIKE1/2 overexpression, we generated stable transgenic Arabidopsis lines overexpressing AUXILIN-LIKE1/2 under the control of chemically inducible promoters. We prepared estradiol-inducible transactivation lines overexpressing untagged AUXILIN-LIKE1 and AUXILIN-LIKE2 (*XVE»AUXILIN-LIKE1* and *XVE»AUXILIN-LIKE2*), as well as a tamoxifen-inducible transactivation line overexpressing GFP-tagged AUXILIN-LIKE1 (*INTAM»GFP-AUXILIN-LIKE1*). Depending on the strength of a particular transgenic line, upon chemical induction, we observed a spectrum of seedling phenotypes ranging from weak reduction in the rates of growth and development to a strong delay or inhibition of germination, as well as the complete inhibition of seedling growth and development if the transgene was activated later (Figures 3A and 3B; Supplemental Figure 4). Overexpression of auxilin-like genes in the lines with strong phenotypes was confirmed with qRT-PCR (Supplemental Figure 5). Using long-term, time-lapse confocal microscopy with automated root tracking (TipTracker; von Wangenheim et al., 2017), we directly compared root growth rates with AUXILIN-LIKE1 expression levels in the root tips of induced *INTAM»GFP-AUXILIN-LIKE1* seedlings (Supplemental Figure 6). GFP-AUXILIN-LIKE1 expression was first observed 1 h after induction and gradually increased until ~15 h. Following GFP-AUXILIN-LIKE1 expression, we observed a sharp decrease in growth between the 4th and 11th hour of induction. Therefore, growth inhibition appears to be a relatively direct effect of AUXILIN-LIKE1/2 overexpression.

Using light microscopy, we found that the morphology of cells in the RAM in AUXILIN-LIKE1/2-overexpressing seedlings was drastically different from that of the wild-type controls. RAM epidermis cells of *XVE»AUXILIN-LIKE1/2* lines exhibited enlarged vacuoles that filled major parts of the cell volume, while the cytosol content was reduced and the nucleus was displaced from its central location (Figures 3C and 3D). This phenomenon was typically observed after ~1 d of induction and became progressively more pronounced after 2 to 3 d.

Inhibition of Endocytosis by AUXILIN-LIKE1/2 Overexpression

Using our inducible overexpressing lines, we then assayed the effect of AUXILIN-LIKE1/2 overexpression on endocytosis. Three lines of evidence support the notion that overexpression of AUXILIN-LIKE1 and AUXILIN-LIKE2 leads to the inhibition of endocytosis: (1) imaging of the endocytic cargoes, (2) imaging of the molecular endocytic machinery, and (3) the distribution of membranes within the cell.

As a basic experiment to assay the general rates of endocytosis, we monitored the uptake of FM4-64, a membrane dye commonly used in studies of endocytosis (Aniento and Robinson, 2005; Bolte et al., 2004; Jelínková et al., 2010). After pulse staining of Arabidopsis seedlings with FM4-64, the dye is gradually taken up by the cell through the endocytic process, and over time it can be observed first at endosomal compartments and then at the tonoplast (vacuolar membrane). *XVE»AUXILIN-LIKE1/2* lines induced overnight (~16–24 h) showed an inhibition of FM4-64 uptake in a majority of the seedlings and RAM epidermis cells observed (Figure 4A). Considering the alteration of cell morphology (the enlargement of vacuoles), we monitored the cells closely in the visible light channel to recognize areas still containing the cytosol, and therefore also endosomes that FM4-64 could reach, and saw that staining was either absent from these areas or endosomes were

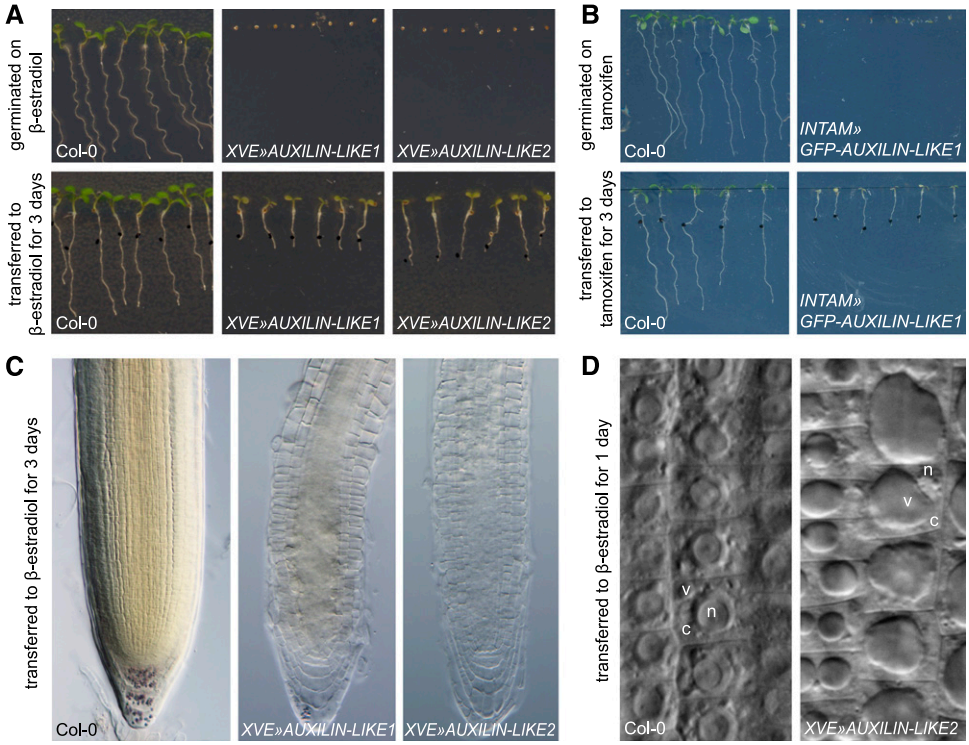

Figure 3. AUXILIN-LIKE1/2 Overexpression Causes an Arrest of Seed Germination and Seedling Growth and Alterations in Cell Morphology.

Overexpression of auxilin-likes in *XVE»AUXILIN-LIKE1/2* **(A)** or *INTAM»GFP-auxilin-like1* **(B)** lines inhibits or strongly delays seed germination and inhibits seedling growth if the transgene is induced postgermination. The RAMs of AUXILIN-LIKE1/2-overexpressing seedlings appear semitransparent **(C)** due to enlargement of vacuoles and reduction of the cytoplasmic volume **(D)**. V, vacuole; c, cytoplasm; n, nucleus.

only weakly stained compared with the controls (Supplemental Figure 7A). In these experiments, we also observed that FM4-64-stained PMs in *XVE»AUXILIN-LIKE1/2* lines often lost the normal, smooth appearance and were instead thicker and uneven, which will be explained below. We then repeated the FM4-64 uptake experiment in the *INTAM»GFP-AUXILIN-LIKE1* line at earlier stages of induction. In this line, we could monitor AUXILIN-LIKE1 expression directly due to the GFP fluorescence. We observed inhibition of FM4-64 uptake into RAM epidermis cells as early as 8 h after transgene induction (Figure 4B). The rate of endocytic tracer uptake was inversely correlated with GFP expression levels on a cell-to-cell basis, demonstrating that the endocytic inhibition by auxilin-like overexpression is cell-autonomous. Importantly, at these early stages of overexpression, the epidermal cells still exhibited normal morphology, with abundant cytosol and small, fragmented vacuoles. Finally, at an even earlier time point of 5 h of expression induction, GFP-AUXILIN-LIKE1 levels were already high in the lateral root cap, and we observed inhibition of FM4-64 uptake specifically in this tissue (Supplemental Figure 7B).

Next, we corroborated these findings by monitoring known CME cargoes, including the auxin efflux transporters of the PIN family (Nodzyński et al., 2016; Adamowski and Friml, 2015) and the syntaxin KNOLLE (Lauber et al., 1997). The endocytic trafficking of PIN proteins is classically assayed via Brefeldin A (BFA) treatments. BFA treatments lead to the deactivation of ADP-ribosylation factors (ARFs), components of the vesicle formation machinery in the endomembrane system, by directly targeting a subset of ARF activators, the guanine nucleotide exchange factors for ARFs (ARF-GEFs). As a result, certain endomembrane trafficking pathways, including GNOM ARF-GEF-dependent polar recycling of PINs to the PM, are inhibited, while others, including PIN endocytosis, are not. As a related phenomenon, agglomeration of endosomal compartments into large structures called "BFA bodies" or "BFA compartments" occurs. Therefore, after BFA treatments, the continuously internalized PIN proteins can be observed inside BFA bodies, from which they cannot be recycled back to the PM (Naramoto et al., 2014). In RAMs of *XVE»AUXILIN-LIKE1/2* seedlings induced for 16 to 24 h, immunolabeled PIN1 was rarely found in BFA bodies in the stele, while in the epidermis, PIN2-GFP was not observed in BFA bodies at all (Figures 5A and 5B), indicating that PIN1 and PIN2 endocytosis was inhibited. To assure that BFA bodies still form after auxilin-like overexpression and that they can be observed despite the enlarged vacuoles, we visualized the BFA body structures themselves using CLC2-GFP as a marker of aggregating endosomal populations (Figure 5C).

To confirm these observations without the use of BFA and to more clearly distinguish the internalization of PIN2 from its biosynthesis and secretion, we monitored the cellular turnover of PIN2 over the long term using PIN2 fused to Dendra (a green-to-red photoactivatable fluorescent protein induced by blue light). After 6 h of *XVE»AUXILIN-LIKE2* induction, we converted PIN2-Dendra from the green into the red form in whole root tips. Eighteen

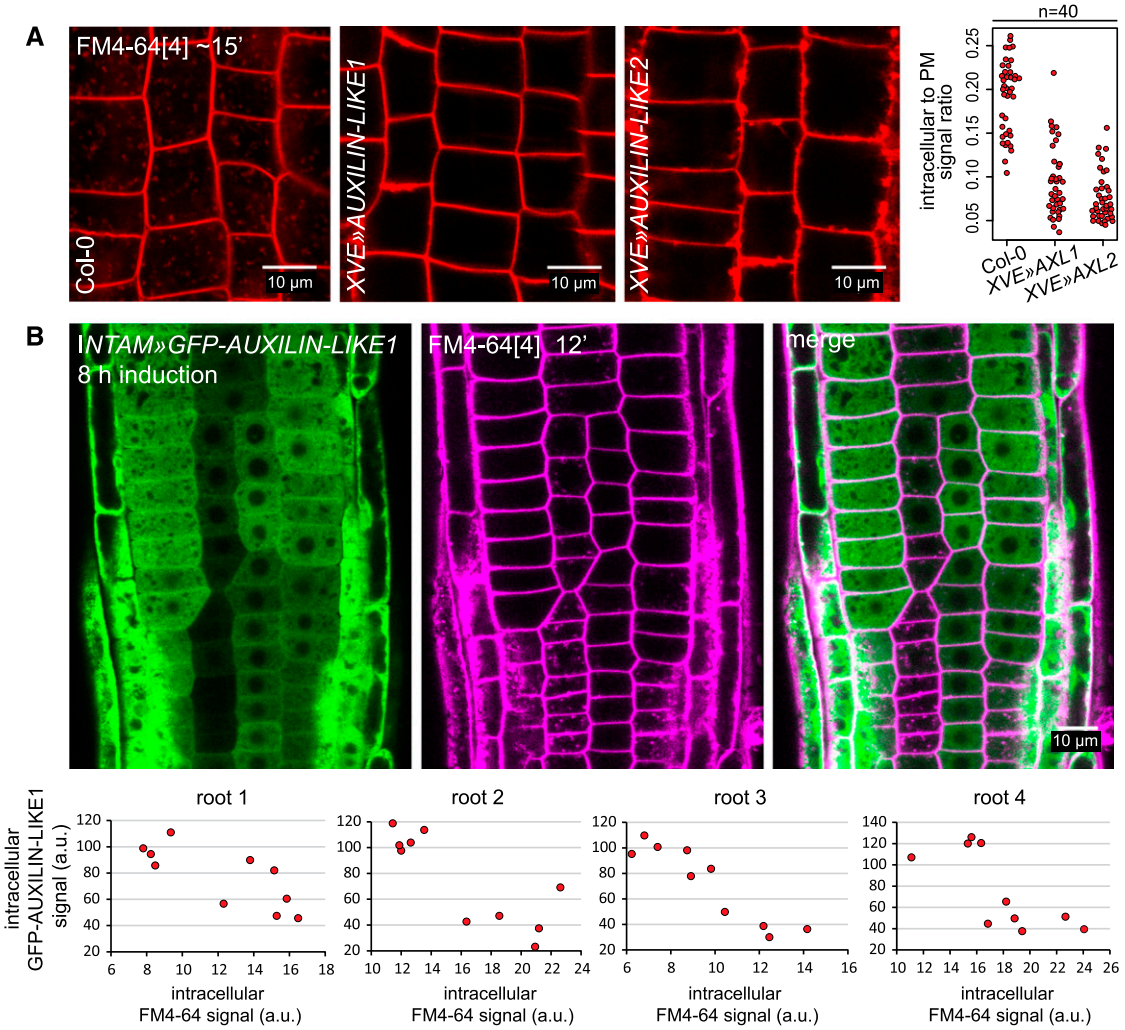

Figure 4. Inhibition of FM4-64 Endocytic Tracer Uptake by AUXILIN-LIKE1/2 Overexpression.

(A) The uptake of the endocytotic tracer FM4-64 into RAM epidermal cells in *XVE»AUXILIN-LIKE1/2* seedlings induced for 16 to 24 h is strongly reduced. At least 10 roots per genotype were imaged in three repeated experiments. The graphs shows quantification of intracellular-to-PM FM4-64 signal ratio from 40 cells coming from four roots in a representative experiment.

(B) FM4-64 uptake at early stages (8 h) of *INTAM»GFP-AUXILIN-LIKE1* induction. The degree of FM4-64 uptake correlated with GFP-AUXILIN-LIKE1 levels in individual root meristem epidermal cells. Graphs show examples of this correlation in four roots. Each data point represents an individual cell. Notice that at this stage of AUXILIN-LIKE1 overexpression, cell morphology remains normal, with abundant cytosol illuminated by GFP-AUXILIN-LIKE1 expression, and small, fragmented vacuoles seen by negative staining. a.u., arbitrary units.

hours later, AUXILIN-LIKE2-overexpressing seedlings retained significant amounts of the red PIN2-Dendra form at the PMs (Figure 5D), demonstrating inhibition of PIN2 endocytosis. In control seedlings, virtually all of the red form became internalized and degraded and was replaced by newly synthesized, green PIN2-Dendra.

In addition to PIN1 and PIN2, we monitored the endocytosis of KNOLLE. KNOLLE is a SNARE protein that is specifically expressed during cell division and targeted to the growing cell plates, where it is retained for some time after cell division is completed. The specific localization of KNOLLE to the newly formed cell membranes is dependent on the endocytic process, as inhibition of endocytosis is associated with lateral spreading of KNOLLE to the "old" PMs after the completion of cell division (Boutté et al., 2010). Similar to previous observations, overexpression of AUXILIN-LIKE1/2 also caused diffusion of KNOLLE out of the newly completed cell membranes and into the old PMs, demonstrating that endocytosis of KNOLLE was inhibited (Figure 5E).

In summary, our imaging of FM4-64 dye, as well as known CME cargoes PIN1, PIN2, and KNOLLE, supported the notion that overexpression of AUXILIN-LIKE1/2 inhibits endocytosis.

AUXILIN-LIKE1/2 Overexpression Inhibits Endocytosis at the Clathrin Recruitment Step

Next, we visualized the effect of auxilin-like overexpression on the molecular components of the endocytic machinery itself. For this

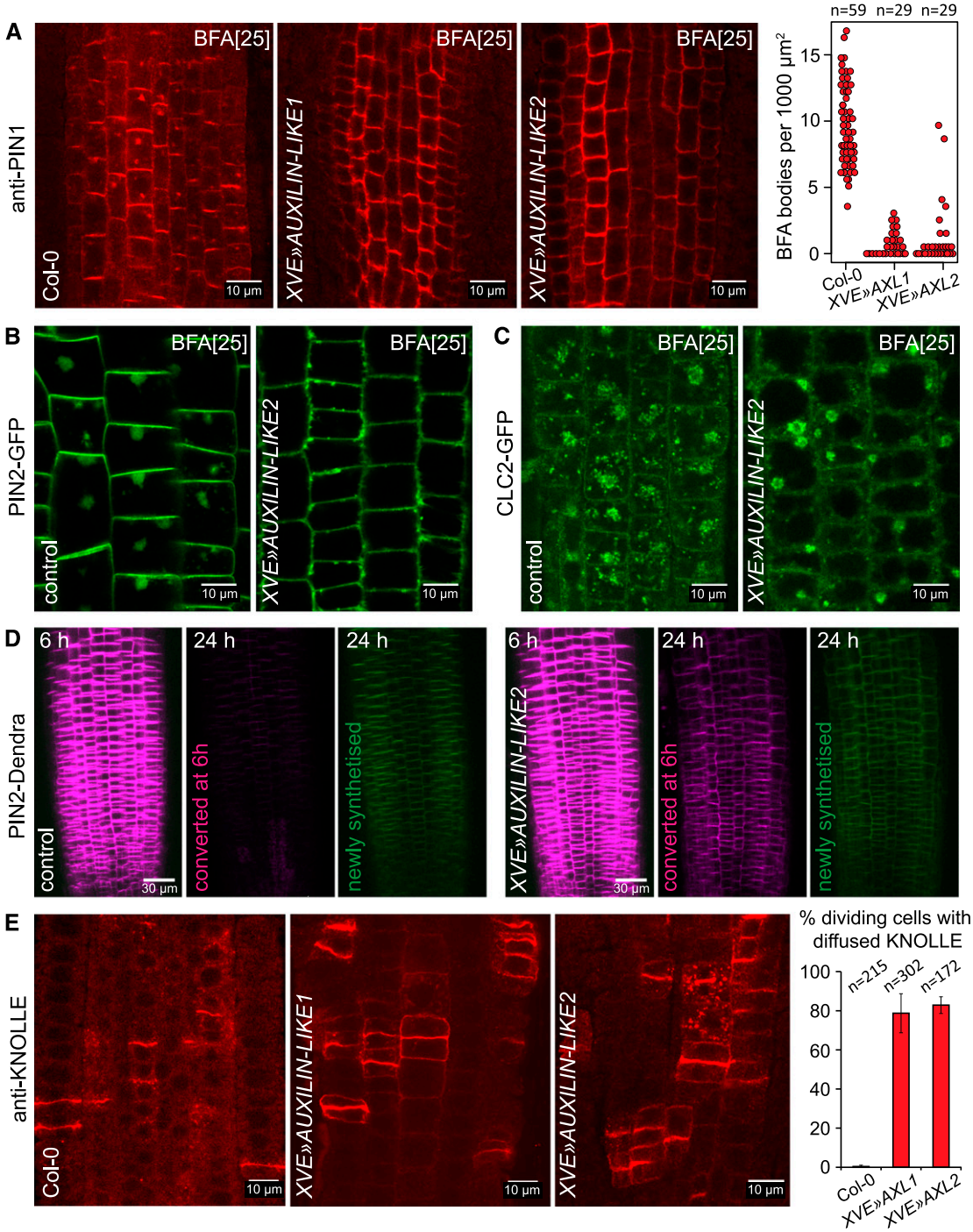

Figure 5. Inhibition of Protein Cargo Endocytosis by AUXILIN-LIKE1/2 Overexpression.

(A) Immunolocalization of PIN1 in the RAM stele after 90 min of BFA (25 μM) treatment. The BFA body number is markedly reduced, indicative of inhibition of PIN1 endocytosis. The graph shows collated results from three repetitions of the experiment. Each data point represents one root.

(B) and **(C)** Following AUXILIN-LIKE2 overexpression, PIN2-GFP does not localize to BFA-induced bodies in RAM epidermis after 90 min of BFA (25 μM) treatment **(B)**. Control experiment with CLC2-GFP used as an endosome marker **(C)** shows that BFA bodies can be easily observed in auxilin-like overexpressing seedlings despite the enlarged vacuoles.

(D) Long-term PIN2 turnover monitoring in *XVE»AUXILIN-LIKE2* with photoconvertible PIN2-Dendra fusion. PIN2-Dendra has been converted from green into red form in whole root tips at 6 h of AUXILIN-LIKE2 induction. At the 24-h time point, significant amounts of the red form have been retained at the PMs of

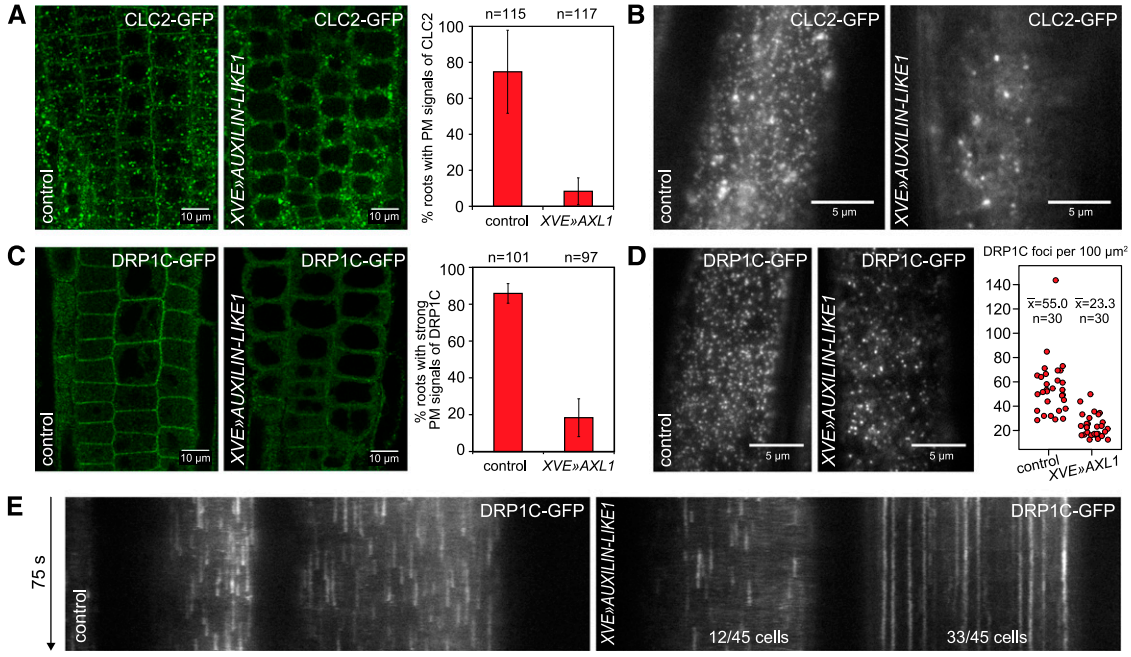

Figure 6. Loss of Clathrin and Dynamin from the PMs of *XVE»AUXILIN-LIKE1* Line.

(A) and **(B)** Following AUXILIN-LIKE1 overexpression, CLC2-GFP signals were absent from the PMs of RAM epidermis cells **(A)** and normal CLC2-GFP endocytic foci could not be observed in hypocotyl epidermis by VAEM **(B)**. The endosomal clathrin populations were retained in both tissues.
(C) to **(E)** DRP1C-GFP PM signals were markedly reduced in RAM epidermis **(C)**, and the density of DRP1C-positive PM foci was reduced in the hypocotyl epidermis **(D)**. The remaining DRP1C-positive PM foci had exceptionally long lifetimes in the majority of observed cells **(E)**.
Graphs in **(A)** and **(C)** show average ± SD percentage of roots with strong PM signals from the fluorescent markers. Graph in **(D)** shows collated measurements from three repetitions of the experiment. All experiments in this figure were performed after 16 to 24 h of *XVE»AUXILIN-LIKE1* induction.

analysis, we crossed the *XVE»AUXILIN-LIKE1* line with fluorescent reporter lines for subunits of the adaptor protein complexes AP2 and TPLATE (AP2A1-TagRFP and TPLATE-GFP), for clathrin (CLC2-GFP), and for dynamins (DRP1C-GFP). We then performed live imaging after 1 d (16–24 h) of AUXILIN-LIKE1 induction.

Through CLSM of seedling roots, we observed that clathrin signals were absent from the PMs of epidermal cells in a majority of AUXILIN-LIKE1-overexpressing seedlings (Figure 6A). These observations were confirmed in the hypocotyl epidermis, where we employed VAEM. Upon AUXILIN-LIKE1 overexpression, normal, densely distributed clathrin-positive PM foci were not observed (Figure 6B). However, we did observe CLC2 signals that were very sparse, larger than normal endocytic pits, and often laterally mobile (Supplemental Movie 2). We cannot determine whether these were clathrin structures that were attached to the PM or localized to the cytosol.

Apart from endocytosis at the PM, clathrin participates in vesicle formation at other compartments of the endomembrane system, where it likely acts with AP-1, AP-3, and AP-4 complexes to function in vacuolar, and potentially secretory, trafficking (Richter et al., 2014; Park et al., 2013; Wang et al., 2013b, 2014; Feraru et al., 2010; Fuji et al., 2016; Robinson and Pimpl, 2014; Zwiewka et al., 2011). Interestingly, it appears that the endosomal clathrin pools were not affected by auxilin-like overexpression, as CLC2-GFP signals were still bound to endosomes (observed as large, intracellular bodies) in both roots and hypocotyls (Figures 6A and 6B; Supplemental Movie 2).

The presence of dynamin (DRP1C) at the PM was also reduced, although the reduction was less pronounced than that of clathrin. In most roots, very weak PM signals of DRP1C-GFP could still be observed (Figure 6C), while VAEM in the hypocotyl epidermis showed DRP1C-positive foci of normal appearance, but at much reduced densities compared with the control (Figure 6D). These remaining DRP1C foci did not show normal dynamics in most of the cells observed, but instead exhibited very long lifetimes, suggesting that these DRP1C-containing structures may have been nonfunctional (Figure 6E).

Figure 5. (continued).

auxilin-like overexpressing seedlings, while the protein has been internalized and degraded in the mock-treated controls. Panels at 6 h show merged green and red channels, while panels at 24 h show green and red channels separately.
(E) Immunolocalization of KNOLLE in the RAM of *XVE»AUXILIN-LIKE* lines showing diffusion of KNOLLE out of the completed cell plates and into the old PM in late cytokinetic cells. The graph shows percentage of cells with diffused KNOLLE signals; error bars indicate SD between 3 experiments.
Experiments in **(A)** to **(C)** and **(E)** were performed after 16 to 24 h of *XVE»AUXILIN-LIKE1/2* induction.

Interestingly, in contrast to clathrin and dynamin, the endocytic adaptor complexes AP2 and TPLATE were not only present at the PMs of *XVE»AUXILIN-LIKE1*, but their binding was consistently stronger than in control conditions. This was most clearly observed in the RAM epidermis using CLSM (Figures 7A and 7B), but the same phenomenon occurred in the hypocotyl epidermis, as observed by VAEM (Figures 7C and 7D). Furthermore, time-resolved imaging demonstrated that these adaptor protein foci had shorter lifetimes at the PM than under control conditions (Figures 7E and 7F; Supplemental Movies 3 and 4).

In summary, live microscopy observations of clathrin, dynamin, and adaptor protein complexes suggest that auxilin-like overexpression blocks endocytosis after the initial step of adaptor protein complex binding to the PM. It appears that endocytic pits are initiated by the adaptors at high frequency, but due to the lack of clathrin binding, they are not progressing and quickly become aborted. The nature of the scarce, remaining DRP1C-positive structures with long lifetimes remains unclear.

Disturbance in Cellular Membrane Distribution Indicates Inhibited Endocytosis

Apart from cargoes and the trafficking-related molecular machinery, the endomembrane system naturally consists of the biological membranes themselves. These membranes are in a constant state of flux through the cell, moving from place to place as vesicles (e.g., secretory vesicles, CCVs, COPI, and COPII-coated vesicles) and through the maturation of compartments, examples of which include the proposed maturation of *trans*-Golgi network/early endosome into multivesicular bodies (Scheuring et al., 2011) and the *cis*-medial-*trans* progression of cisternae in the Golgi stack. Considering this overall membrane flow, one can imagine that interfering with a particular trafficking process could lead to broad changes in membrane distribution in the endomembrane system. Specifically, inhibited endocytosis should lead to the excess accumulation of the membrane at the cell periphery—the plasma membrane—and a concomitant loss of membranes from the cell interior, both occurring due to the now isolated, imbalanced activity of the secretory pathway. Indeed, upon staining the PMs in AUXILIN-LIKE1/2-overexpressing lines with the FM4-64 dye or with PIN2-GFP, we observed thick deposits of membrane at the cell periphery instead of the typical smooth, thin PMs (Figure 8). This observation provides more, although indirect, evidence for inhibited endocytosis due to AUXILIN-LIKE1/2 overexpression. Staining with propidium iodide showed that the cell wall structure was also affected (Supplemental Figure 8), as thick deposits strongly binding to propidium iodide could be seen.

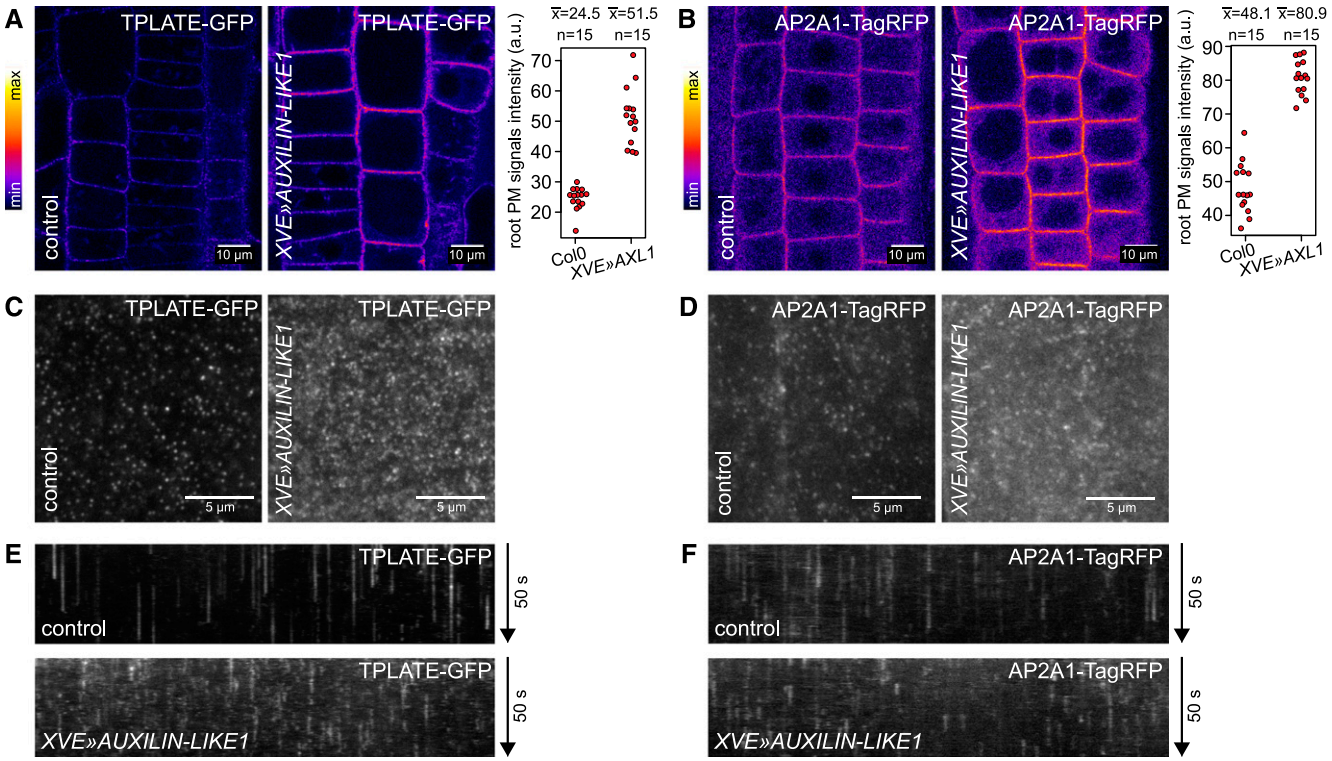

Figure 7. Increased PM Binding of Endocytic Adaptor Protein Complexes in *XVE»AUXILIN-LIKE1* Line.

Overexpression of AUXILIN-LIKE1 caused increased PM binding of TPLATE, a subunit of the TPLATE complex, as well as AP2A1, a subunit of the AP-2 complex. CLSM images from RAM epidermis (**[A]** and **[B]**) and VAEM images from hypocotyl epidermis (**[C]** and **[D]**) are shown. Graphs in **(A)** and **(B)** show PM signal intensity measurements from a representative experiment. Kymographs (**[E]** and **[F]**) show reduced lifetimes of TPLATE and AP2A1 foci in *XVE»AUXILIN-LIKE1* line, likely indicating that endocytic pits aborted after initiation. All experiments in this figure were performed after 16 to 24 h of *XVE»AUXILIN-LIKE1* induction.

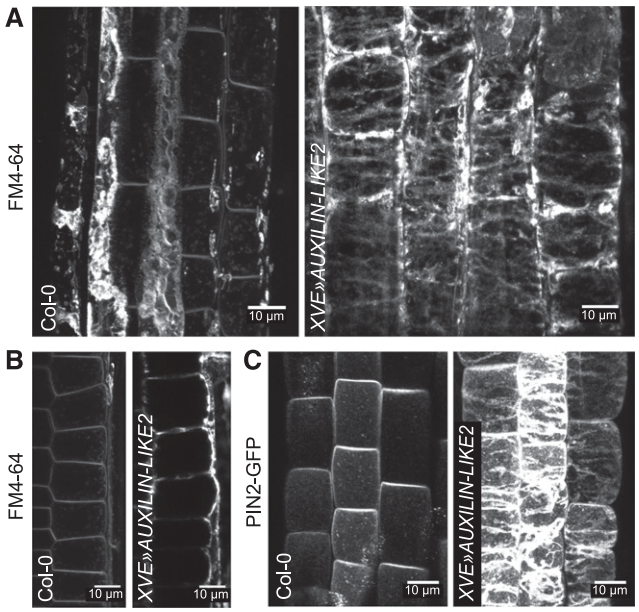

Figure 8. Excess Membrane Accumulation at the PM as a Result of Inhibited Endocytosis.

Overexpression of AUXILIN-LIKE2 caused excess deposition of membrane material at the PMs of root epidermis, as visualized with FM4-64 staining (**[A]** and **[B]**) or with PIN2-GFP **(C)**. **(A)** and **(C)** are maximum intensity projections of *z*-stacks through outer region of the epidermis, while **(B)** is a longitudinal section of epidermal cells showing membrane aggregation mainly in the outer domain. FM4-64-stained deposits in Col-0 in **(A)** are likely remnants of apoptosed lateral root cap cells.

Taken together, the imaging of endocytic cargoes, the endocytic machinery components, and the cellular distribution of membranes all demonstrated that overexpressing AUXILIN-LIKE1/2 leads to the inhibition of endocytosis. This phenomenon is analogous to the effect of overexpression of auxilin homologs in non-plant systems. However, we do not consider these data to necessarily be indicative of a vesicle-uncoating function of AUXILIN-LIKE1/2. The most parsimonious interpretation is that overexpressed AUXILIN-LIKE1/2 proteins may inhibit the recruitment of clathrin to initiating endocytic pits simply by binding to and retaining all available clathrin in the cytosol, although this simple model would not explain why the endosomal pools of clathrin remain intact (Figures 6A and 6B). While not proving a specific function in uncoating, these findings, together with our protein-protein interaction and subcellular localization data, constitute strong evidence for a clathrin-related function of AUXILIN-LIKE1/2.

AUXILIN-LIKE1/2 Loss of Function

In an attempt to address the specific molecular function of AUXILIN-LIKE1/2, we aimed to obtain *auxilin-like1/2* knockout plants. The behaviors of the two proteins in terms of interactions, localization, and the effects of overexpression were the same in our experiments, and the two proteins share very high sequence similarity. Therefore, we expected AUXILIN-LIKE1 and AUXILIN-LIKE2 to be functionally redundant, so we aimed to obtain a double mutant. *AUXILIN-LIKE1* and *AUXILIN-LIKE2* genes occupy a common locus on chromosome 4, in which their coding sequences are inversely oriented around a short, shared promoter region (Figure 9A). The genes are therefore tightly linked, making it impossible to generate double mutants by crossing single T-DNA insertion lines. Instead, we generated double knockouts by simultaneously targeting both homologs using CRISPR technology. The CRISPR method generates short (1–2 nucleotide) deletions or insertions in the target sequence, thus causing open reading frame shifts and disrupting the coding sequence. Using this approach, we isolated two double mutant combinations, *auxilin-like1/2*^{c1} and *auxilin-like1/2*^{c2}, as well as single *auxilin-like1* and *auxilin-like2* mutants (Figure 9A). To our surprise, both the single and the double mutants were phenotypically normal under standard growth conditions at the seedling and adult stages (Figure 9B). The plants also exhibited normal fertility. Furthermore, an FM4-64 uptake experiment using the RAM epidermis of *auxilin-like1/2*^{c1} seedlings did not indicate any defects in endocytosis (Figure 9C). This loss-of-function analysis revealed that Arabidopsis auxilin-like proteins are not essential for endocytosis and development, at least under optimal environmental conditions. This finding is in contrast to the results of similar analyses in animals such as mouse (*Mus musculus*), worm (*Caenorhabditis elegans*), and zebra fish (*Danio rerio*), where defects in growth and development of auxilin/GAK mutants were reported (Yim et al., 2010; Greener et al., 2001; Bai et al., 2010; Lee et al., 2008), hinting at crucial differences in the mechanism of clathrin-mediated endocytosis between plants and animals.

DISCUSSION

Here, we aimed to expand our knowledge of clathrin-mediated endocytosis in plants by searching for, and functionally characterizing, novel clathrin-associated proteins. Using a TAP-MS approach, we identified four CLC binding proteins with possible endocytic functions: CAP1, SH3P2, AUXILIN-LIKE1, and AUXILIN-LIKE2. We analyzed the binary interactions among these proteins and revealed their localization to the PM and the cell plate, two of the sites of clathrin action.

Our more detailed studies focused on characterizing the two putative uncoating factor homologs, AUXILIN-LIKE1 and AUXILIN-LIKE2. Like auxilin homologs in non-plants, we found that overexpressing AUXILIN-LIKE1/2 led to an inhibition of endocytosis. We believe that our inducible auxilin-overexpressing lines are useful and very efficient genetic tools for specifically interfering with endocytosis, with applications in studies of various clathrin-dependent processes (Ortiz-Morea et al., 2016). Our in-depth mapping of the effects of AUXILIN-LIKE1 overexpression on the molecular components of the endocytic pathway may prove interesting for researchers interested in the endocytic process itself. We note that the effect of AUXILIN-LIKE1/2 overexpression appears to be specific for the PM pool of clathrin, as we did not observe a loss of clathrin from the endosomal compartments.

The observation that membranes accumulated at the cell periphery, which we interpret as an effect of the continuation of secretion in the absence of endocytosis, tangibly demonstrates the interdependence of distinct trafficking processes in the endomembrane system. Although highly speculative, it is tempting to

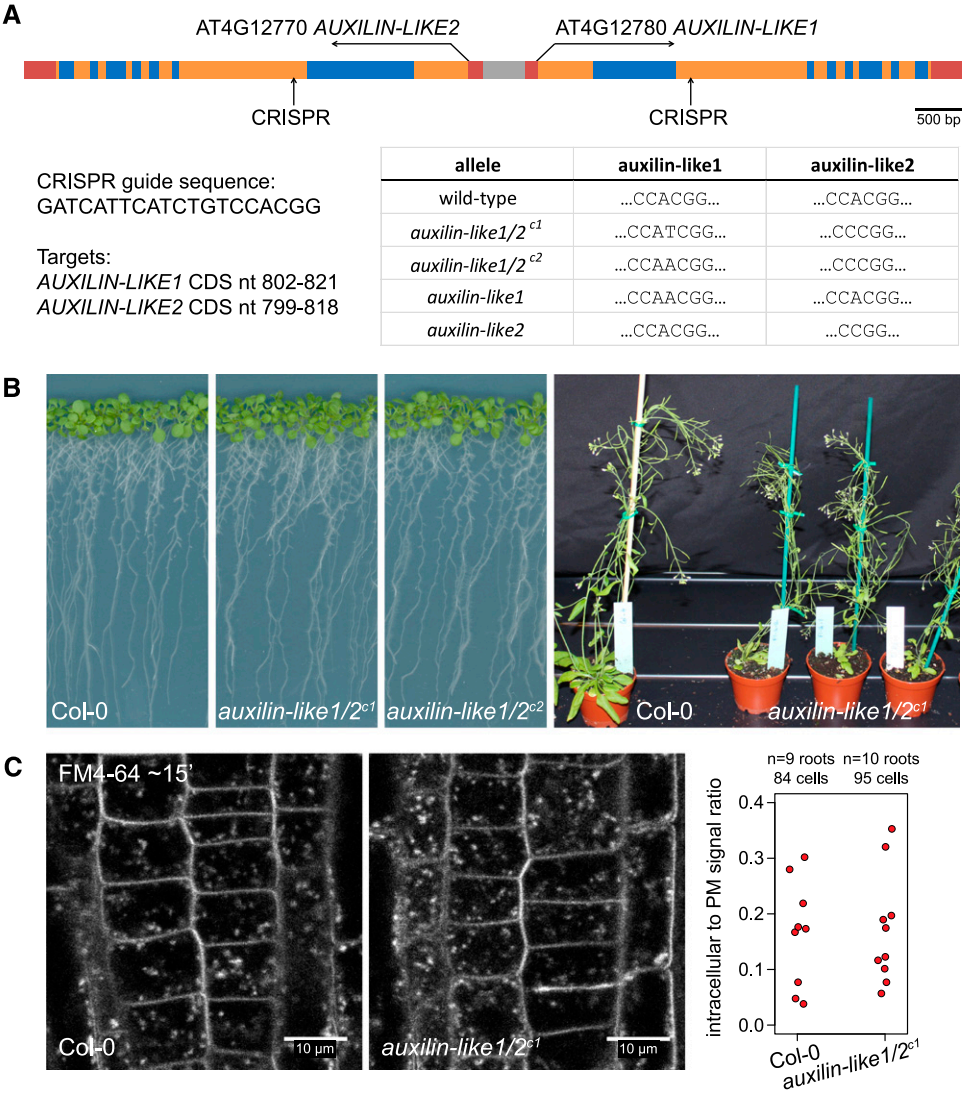

Figure 9. *auxilin-like1/2* Loss-of-Function Mutants.

(A) Isolation of *auxilin-like1/2* CRISPR mutants. Top: Overview of the *AUXILIN-LIKE1/2* genomic locus showing CRISPR target sites in the second exons of *AUXILIN-LIKE1* and *AUXILIN-LIKE2*. Bottom: Details of the CRISPR target sequence and the isolated mutant alleles.
(B) *auxilin-like1/2* double homozygous mutants, as well as single mutants, developed normally at both the seedling and adult stages.
(C) FM4-64 uptake into *auxilin-like1/2*^{c1} seedlings was comparable to that of the controls, indicating functional endocytosis.

hypothesize that the loss of cytoplasm in which the endomembrane compartments are embedded, together with the increase in vacuolar volume, as observed in AUXILIN-LIKE1/2-overexpressing lines, are also trafficking homeostasis-related phenomena, as they may represent secondary effects of the bulk loss of internal endomembrane compartments.

In an attempt to address the specific molecular function of AUXILIN-LIKE1/2, we also generated *auxilin-like1/2* mutants using CRISPR technology. We found that the loss of AUXILIN-LIKE1/2 function did not visibly affect endocytosis or plant growth and development under optimal growth conditions. This is in contrast to loss-of-function alleles of other endocytic components, which exhibit various defects in growth, development, and/or reduced fertility (Gadeyne et al., 2014; Kang et al., 2001, 2003; Collings et al., 2008; Kim et al., 2013; Kitakura et al., 2011). This observation also differs from that of auxilin loss-of-function mutants in yeast, whose growth is reduced (Ding et al., 2015), and auxilin/GAK loss-of-function mutants in animals such as mouse, worm, or zebra fish, where various aspects of development are affected (Yim et al., 2010; Greener et al., 2001; Bai et al., 2010; Lee et al., 2008).

We propose several possible interpretations for the lack of mutant phenotypes in *auxilin-like1/2*. First, it appears likely that AUXILIN-LIKE1/2 function is necessary for only a small subset of all clathrin-coated vesicles that form at the PM. This can be concluded from our VAEM colocalization analysis of clathrin and AUXILIN-LIKE1, in which we observed that a vast majority of

CCPs did not recruit AUXILIN-LIKE1. As discussed above, it is possible that auxilin-like recruitment often takes place in the cytosol, and such events could have been missed by our imaging system. However, it is also possible that most CCVs are in fact uncoated with the help of other factors, while the function of AUXILIN-LIKE1/2 is limited to only a specific subpopulation of vesicles. This appears consistent with the observation that knocking out the two genes does not visibly interfere with endocytosis, and it hints at the exciting possibility of the existence of functionally distinct populations of PM-derived CCVs in plant cells, only one of which uses the conserved auxilin-Hsc70 pathway for uncoating.

Second, the lack of evident phenotypes in *auxilin-like1/2* may be explained by a functional overlap between the closely homologous AUXILIN-LIKE1/2 pair and any of the five remaining auxilin-like proteins in Arabidopsis. However, we and others identify these proteins as auxilin-like only due to the presence of C-terminal DNAJ domains that recruit and activate the heat shock protein. The remaining portions of auxilin-likes have different lengths and bear little or no sequence similarity when comparisons are made between the closely homologous AUXILIN-LIKE1/2 pair and AUXILIN-LIKE3-7 (Supplemental Figure 9). The lack of sequence similarity, together with the specific detection of AUXILIN-LIKE1/2 but not AUXILIN-LIKE3-7 in our CLC-TAP assay, suggest a possible diversification in the functions of plant C-terminal DNAJ proteins beyond simply clathrin-related processes. An example of this is JAC1 (AUXILIN-LIKE6), which was identified in a forward genetic screen for regulators of light-dependent chloroplast relocations in the leaf (Suetsugu et al., 2005), a process, to our knowledge, not regulated by clathrin. An analysis of the effects of AUXILIN-LIKE3-7 overexpression, as well as clathrin binding assays, may help to address with more certainty whether any of these proteins could function in the endocytic process together with AUXILIN-LIKE1/2. At the moment, we hypothesize that plant cells recruit the chaperoning function of Hsc70 at various cellular locations using a suite of auxilin-like DNAJ domain proteins that act as binding adaptors between the chaperone and distinct target protein complexes.

As a final note, while it is true that some of the features of AUXILIN-LIKE1/2, such as the presence of a C-terminal DNAJ domain, the late recruitment to coated pits, and the effects of overexpression, suggest they possess a function identical to that of non-plant auxilins, our data are insufficient to draw specific conclusions about the molecular function of these auxilin-like proteins. Returning to protein sequence comparisons, when whole sequences are taken into consideration, neither AUXILIN-LIKE1/2 nor any other Arabidopsis auxilin-like are similar to non-plant auxilins; interestingly, yeast auxilin is overall not similar to animal auxilins either. Although biochemical experiments have suggested that AUXILIN-LIKE1 possesses uncoating activity in vitro (Lam et al., 2001), we believe that further investigation into the molecular function of AUXILIN-LIKE1/2 and into the uncoating of CCVs in plants, may bring more clarity. The recent finding that the yeast auxilin homolog AUX1/SWA2 not only participates in the uncoating of CCVs, but also functions with COPI and COPII-coated vesicles in the early secretory pathway (Ding et al., 2015), provides a cautionary tale against assuming that distantly similar proteins found across the tree of life possess identical molecular functions.

METHODS

Plant Materials

The following previously published *Arabidopsis thaliana* lines were used: *UBQ10$_{pro}$:SH3P2-GFP* (Zhuang et al., 2013), *PIN2$_{pro}$:PIN2-GFP* (Abas et al., 2006), *PIN2$_{pro}$:PIN2-Dendra* (Salanenka et al., 2018), *CLC2$_{pro}$:CLC2-GFP* and *DRP1C$_{pro}$:DRP1C-GFP* (Konopka and Bednarek, 2008), *INTAM:GAL4* (Friml et al., 2004), *TPLATE-GFP* × *AP2A1-TagRFP* (Gadeyne et al., 2014), and *35S$_{pro}$:PIN5-GFP* (Mravec et al., 2009).

The following lines and crosses were generated in this study: *XVE»AUXILIN-LIKE1*, *XVE»AUXILIN-LIKE2*, *XVE»AUXILIN-LIKE1×CLC2$_{pro}$:CLC2-GFP*, *XVE»AUXILIN-LIKE1×DRP1C$_{pro}$:DRP1C-GFP*, *XVE»AUXILIN-LIKE1×TPLATE-GFP*, *XVE»AUXILIN-LIKE1×AP2A1-TagRFP*, *XVE»AUXILIN-LIKE2×PIN2$_{pro}$:PIN2-GFP*, *XVE»AUXILIN-LIKE2×PIN2$_{pro}$:PIN2-Dendra*, *CAP1$_{pro}$:CAP1-mCherry*, *35S$_{pro}$:CAP1-RFP*, *35S$_{pro}$:SH3P2-GFP*, *UBQ10$_{pro}$:GFP-AUXILIN-LIKE1*, *CLC2$_{pro}$:CLC2-GFP×UBQ10$_{pro}$:mCherry-AUXILIN-LIKE1*, *35S$_{pro}$:RFP-AUXILIN-LIKE1*, *35S$_{pro}$:RFP-AUXILIN-LIKE2*, *UAS:GFP-AUXILIN-LIKE1*, *INTAM»GFP-AUXILIN-LIKE1* (*UAS:GFP-AUXILIN-LIKE1×''' INTAM:GAL4*), *auxilin-like1/2^{c1}*, *auxilin-like1/2^{c2}*, *auxilin-like1*, and *auxilin-like2*.

Unfortunately, *35S$_{pro}$:RFP-auxilin-like1/2* seeds are not available due to low yields and a high degree of silencing, but expression vectors for plant transformation can be provided instead.

Molecular Cloning

All constructs used for TAP, for generating stable Arabidopsis transgenic lines, and for BiFC assays were cloned with the Gateway system. The following Gateway entry clones were generated in this study: CLC1/pDONR221, AUXILIN-LIKE1/pENTR/D-TOPO, AUXILIN-LIKE2/pENTR/D-TOPO, AUXILIN-LIKE1/pDONRP2rP3, AUXILIN-LIKE2/pDONRP2rP3, CAP1/pENTR/D-TOPO, SH3P2/pENTR/D-TOPO (all in variants with and without stop codons), PIP5K1/pDONR221, and pCAP1/pDONRP4P1r. The coding sequences of *CLC1*, *AUXILIN-LIKE1*, *AUXILIN-LIKE2*, and *CAP1* were cloned from Arabidopsis (accession Columbia-0) cDNA, whereas those of *SH3P2* and the *CAP1* promoter were cloned from Arabidopsis Col-0 genomic DNA. The primers used are shown in Supplemental Table 1.

The expression vectors were cloned using previously published Gateway vectors (Karimi et al., 2002; Curtis and Grossniklaus, 2003; Van Leene et al., 2014). Constructs for TAP were generated by fusing CLC1 with TAP tags and with 35S promoter sequences in pKCTAP and pKCTAP destination vectors. The following constructs were cloned and used for stable transformation of Arabidopsis: *XVE»AUXILIN-LIKE1* and *XVE»AUXILIN-LIKE2* [pMDC7B(UBQ10)], *35S$_{pro}$:RFP-AUXILIN-LIKE1* and *35S$_{pro}$:RFP-AUXILIN-LIKE2* (pK7WGR2), *UAS:GFP-AUXILIN-LIKE1* (pK7m34GW), *UBQ10$_{pro}$:GFP-AUXILIN-LIKE1* (pB7m34GW,0), *UBQ10$_{pro}$:mCherry-AUXILIN-LIKE1* (pB7m34GW,0), *35S$_{pro}$:SH3P2-GFP* (pH7FWG2), *35S$_{pro}$:CAP1-RFP* (pK7RWG2), and *CAP1$_{pro}$:CAP1-mCherry* (pK7m34GW). The constructs used for the BiFC assays were cloned in p*7m34GW and p*7m24GW2 backbones (where * indicates resistance cassettes not relevant for these constructs) and consisted of fusions of N- and C-terminal parts of EGFP fused to CLC1, AUXILIN-LIKE1, AUXILIN-LIKE2, CAP1, SH3P2, and PIP5K1, all under the control of the 35S promoter.

TAP

TAP using CLC1 as bait was performed as described previously (Van Leene et al., 2014) with Arabidopsis cell cultures.

BiFC Assays

For the BiFC assays, *Nicotiana benthamiana* leaves were transiently transformed with *Agrobacterium tumefaciens*. The Agrobacterium strains carrying the BiFC constructs were grown to OD = 1, spun down, and

resuspended in infiltration buffer (10 mM $MgCl_2$, 10 mM MES, and 100 μM acetosyringone) to OD = 1.5. The suspensions were incubated at room temperature on a shaker for 2 h. Strains carrying the two assayed constructs were mixed and injected into the bottom sides of leaves. Leaves were imaged by CLSM 3 to 4 d after injection. Each interacting pair was assayed in three repeated experiments. Positive interactions displayed broad areas of GFP fluorescence throughout the injected leaf surface. Single photographs of GFP fluorescence were taken to document the results.

Growth Conditions and Chemical Induction of Transgenes

Arabidopsis seedlings were grown on half-strength Murashige and Skoog (1/2MS) medium with 1% (w/v) sucrose at 21°C under a 16-h-day/8-h-night cycle or in darkness for imaging in etiolated hypocotyls. Lights used were Philips GreenPower LED in deep red/far red/blue combination, intensity: 2100 μW ±10%. Estradiol induction of the *XVE»AUXILIN-LIKE1/2* lines was done by transferring 3-d-old seedlings to medium containing β-estradiol (Sigma-Aldrich) or solvent (ethanol) as a control. β-Estradiol concentrations used were 2.5 μg/mL (~9.18 μM) for experiments presented in Figures 3, 4, 5A to 5C, 5E, 6 to 8, and Supplemental Figure 7A and 2 μM for experiments presented in Figure 5D and Supplemental Figures 5 and 8. Induction of the *INTAM»GFP-AUXILIN-LIKE1* line was done analogously on medium supplemented with 2 μM tamoxifen (Sigma-Aldrich).

Seedling Root Morphology

For light microscopy of *XVE»AUXILIN-LIKE1/2* seedling roots, seedlings were stained in Lugol's solution for ~1 min, washed, and mounted on slides in chloral hydrate solution.

Immunostaining

An Intavis InsituPro VSi robot was used for immunostaining according to a previously published protocol (Sauer et al., 2006). The following antibodies were used: rabbit anti-PIN1 (1:1000; Paciorek et al., 2005), rabbit anti-PIN2 (1:1000; Abas et al., 2006), rabbit anti-KNOLLE (1:1000; Lauber et al. 1997), and anti-rabbit-Cy3 (1:600; Sigma-Aldrich; catalog no. C2306).

Fluorescent Imaging

CLSM imaging was done with a Zeiss LSM700, LSM800, and LSM880 confocal microscopes with Plan-Apochromat 20x/0.8 and Plan-Apochromat 40×/1.2 lenses. Long-term live imaging with root growth tracking was performed on a vertical Zeiss LSM700 as previously described (von Wangenheim et al., 2017).

VAEM imaging was performed with an Olympus IX83 inverted microscope equipped with a cell-TIRF module and an UAPON OTIRF 100× lens. For colocalization imaging of $CLC2_{pro}$*:CLC2-GFP*×$UBQ10_{pro}$*:mCherry-AUXILIN-LIKE1*, the two channels were captured sequentially.

FM4-64 and FM1-43 Staining

For FM4-64 uptake experiments, seedlings were stained in liquid 1/2MS medium with 1% (w/v) sucrose supplemented with 2 μM FM 4-64 dye (Thermo Fisher) for 5 min in the dark and on ice. Excess dye was washed off and the seedlings were mounted in 1/2MS medium with 1% (w/v) sucrose on microscopy slides at room temperature, marking the start of the internalization time measurement.

To visualize the membrane accumulation at the PMs of the *XVE»AUXILIN-LIKE2* line, and for colocalizations of fluorescent markers with PM-localized FM4-64 and FM1-43 stains, the seedlings were treated as described above but at room temperature and imaged immediately after washing. FM1-43 stain was used at 0.2 μM concentration.

BFA Treatments

Seedlings were incubated in liquid 1/2MS medium with 1% (w/v) sucrose and containing BFA (Sigma-Aldrich) at a final concentration of 25 μM. The solvent (DMSO) was added to the controls.

Propidium Iodide Staining

Propidium iodide (Sigma-Aldrich) was diluted 100× in 1/2MS medium with 1% (w/v) sucrose and roots were stained for 2 min before CLSM imaging.

Fluorescence Quantification

Quantification of CLSM and VAEM fluorescence images was performed using Fiji/ImageJ. FM4-64 uptake was quantified by comparing average PM and intracellular signal intensities in individual cells. BFA bodies stained by PIN1 were counted in circular areas 50 μm in diameter, placed in the middle of microscopic pictures. DRP1C-GFP foci at the PM in VAEM pictures were counted similarly in circular areas 120 pixels in diameter. PM signal intensities of TPLATE-GFP and AP2A1-TagRFP in root epidermis were measured on lines drawn along multiple PMs in individual microscopic pictures.

Quantitative RT-PCR

Total RNA from ~15 4-d-old seedlings induced with 2 μM β-estradiol/4-hydroxytamoxifen/solvent control (Sigma-Aldrich) for 24 h was extracted using the TRIzol reagent (Invitrogen) and purified using an RNeasy Mini Kit (Qiagen) according to manufacturer's instructions. Two micrograms of RNA was reverse-transcribed using an iScript cDNA Synthesis Kit (Bio-Rad). qRT-PCR was performed in 5-μL reactions using the LightCycler480 SYBR Green I Master Mix in a LightCycler480 II (ser. no. 5659; Roche) according to the manufacturer's instructions. Relative gene expression was calculated with the $2^{-\Delta\Delta CT}$ method (Livak and Schmittgen, 2001). The primers used are listed in Supplemental Table 1.

CRISPR Mutant Isolation

The CRISPR construct was cloned according to a published method (J. Richter, J.M. Watson, P. Stasnik, M. Borowska, J. Neuhold, P. Stolt-Bergner, V.K. Schoft, and M.T. Hauser, unpublished data). T1 plants transformed with the CRISPR construct were selected on Basta and resistant transformants genotyped for *AUXILIN-LIKE1/2* mutations by PCR amplification and sequencing of relevant gene fragments. Plants carrying mutations in auxilin-like paralogs were propagated, and the T2 progenies were PCR genotyped to find those that segregated out the CRISPR cassette (by amplification of the *Cas9* and *Bar* genes). Among them, single and double *auxilin-like* homozygotes were selected. The primers used are listed in Supplemental Table 1.

Protein Sequence Alignment

Auxilin-like protein sequences were aligned using the Geneious software package (www.geneious.com) with standard settings.

Accession Numbers

Sequence data from this article can be found in the GenBank/EMBL libraries under the following accession numbers: AUXILIN-LIKE1 (At4g12780), AUXILIN-LIKE2 (At4g12770), CAP1 (At4g32285), SH3P2 (At4g34660), CLC1 (At2g20760), CLC2 (At2g40060), CHC1 (At3g08530), CHC2 (At3g11130), DRP1C (At1g14830), TPLATE (At3g01780), AP2A1 (At5g22770), KNOLLE (At1g08560), PIN1 (At1g73590), PIN2 (At5g57090), AUXILIN-LIKE3 (At1g21660), AUXILIN-LIKE4 (At4g36520), AUXILIN-

LIKE5 (At1g75310), JAC1/AUXILIN-LIKE6 (At1g75100), AUXILIN-LIKE7 (At1g30280), PIP5K1 (At1g21980), and DHNAT2 (At5g48950).

Supplemental Data

Supplemental Figure 1. Additional BiFC interactions.

Supplemental Figure 2. Additional subcellular localization data for AUXILIN-LIKEs, SH3P2, and CAP1.

Supplemental Figure 3. Growth and development of seedlings in transgenic lines constitutively overexpressing AUXILIN-LIKE1, SH3P2, and CAP1.

Supplemental Figure 4. Uninduced controls for seed germination experiments with *XVE»AUXILIN-LIKE* lines.

Supplemental Figure 5. qPCR of inducible AUXILIN-LIKE overexpression lines.

Supplemental Figure 6. Correlation of GFP-AUXILIN-LIKE1 expression and root growth inhibition during *INTAM»GFP-AUXILIN-LIKE1* induction.

Supplemental Figure 7. Additional data on FM4-64 uptake in inducible AUXILIN-LIKE overexpression lines.

Supplemental Figure 8. Propidium iodide staining of *XVE»AUXILIN-LIKE2* roots.

Supplemental Figure 9. Protein sequence alignment of Arabidopsis AUXILIN-LIKE1-7.

Supplemental Table 1. Primers used in this study.

Supplemental Movie 1. VAEM colocalization of CLC2-GFP and mCherry-AUXILIN-LIKE1.

Supplemental Movie 2. VAEM imaging of CLC2-GFP in the *XVE»AUXILIN-LIKE1* line.

Supplemental Movie 3. VAEM imaging of TPLATE-GFP in the *XVE»AUXILIN-LIKE1* line.

Supplemental Movie 4. VAEM imaging of AP2A1-TagRFP in the *XVE»AUXILIN-LIKE1* line.

ACKNOWLEDGMENTS

We thank James Matthew Watson, Monika Borowska, and Peggy Stolt-Bergner at ProTech Facility of the Vienna Biocenter Core Facilities for the CRISPR/CAS9 construct; Anna Müller for assistance with molecular cloning; Sebastian Bednarek, Liwen Jiang, and Daniël Van Damme for sharing published material; Matyáš Fendrych, Daniël Van Damme, and Lindy Abas for valuable discussions; and Martine De Cock for help with correcting the manuscript. This work was supported by the European Research Council under the European Union Seventh Framework Programme (FP7/2007-2013)/ERC Grant 282300 and by the Ministry of Education of the Czech Republic/MŠMT project NPUI-LO1417.

AUTHOR CONTRIBUTIONS

All authors designed parts of the research. M.A., M.N., U.K., and M.G. performed experiments. M.A. and J.F. wrote the manuscript.

Received October 9, 2017; revised January 16, 2018; accepted March 5, 2018; published March 6, 2018.

REFERENCES

Abas, L., Benjamins, R., Malenica, N., Paciorek, T., Wiśniewska, J., Moulinier–Anzola, J.C., Sieberer, T., Friml, J., and Luschnig, C. (2006). Intracellular trafficking and proteolysis of the *Arabidopsis* auxin-efflux facilitator PIN2 are involved in root gravitropism. Nat. Cell Biol. **8:** 249–256.

Adamowski, M., and Friml, J. (2015). PIN-dependent auxin transport: action, regulation, and evolution. Plant Cell **27:** 20–32.

Ahle, S., and Ungewickell, E. (1990). Auxilin, a newly identified clathrin associated protein in coated vesicles fron bovine brain. J. Cell Biol. **111:** 19–29.

Ahn, G., et al. (2017). SH3P2 plays a crucial role at the step of membrane tubulation during cell plate formation in plants. Plant Cell **29:** 1388–1405.

Aniento, F., and Robinson, D.G. (2005). Testing for endocytosis in plants. Protoplasma **226:** 3–11.

Bai, T., Seebald, J.L., Kim, K.-E., Ding, H.-M., Szeto, D.P., and Chang, H.C. (2010). Disruption of zebrafish cyclin G-associated kinase (GAK) function impairs the expression of Notch-dependent genes during neurogenesis and causes defects in neuronal development. BMC Dev. Biol. **10:** 7.

Bashline, L., Li, S., Anderson, C.T., Lei, L., and Gu, Y. (2013). The endocytosis of cellulose synthase in *Arabidopsis* is dependent on μ2, a clathrin-mediated endocytosis adaptin. Plant Physiol. **163:** 150–160.

Ben Khaled, S., Postma, J., and Robatzek, S. (2015). A moving view: subcellular trafficking processes in pattern recognition receptor–triggered plant immunity. Annu. Rev. Phytopathol. **53:** 379–402.

Bolte, S., Talbot, C., Boutte, Y., Catrice, O., Read, N.D., and Satiat-Jeunemaitre, B. (2004). FM-dyes as experimental probes for dissecting vesicle trafficking in living plant cells. J. Microsc. **214:** 159–173.

Boucrot, E., Ferreira, A.P.A., Almeida-Souza, L., Debard, S., Vallis, Y., Howard, G., Bertot, L., Sauvonnet, N., and McMahon, H.T. (2014). Endophilin marks and controls a clathrin-independent endocytic pathway. Nature **517:** 460–465.

Boutté, Y., Frescatada-Rosa, M., Men, S., Chow, C.-M., Ebine, K., Gustavsson, A., Johansson, L., Ueda, T., Moore, I., Jürgens, G., and Grebe, M. (2010). Endocytosis restricts *Arabidopsis* KNOLLE syntaxin to the cell division plane during late cytokinesis. EMBO J. **29:** 546–558.

Collings, D.A., Gebbie, L.K., Howles, P.A., Hurley, U.A., Birch, R.J., Cork, A.H., Hocart, C.H., Arioli, T., and Williamson, R.E. (2008). *Arabidopsis* dynamin-like protein DRP1A: A null mutant with widespread defects in endocytosis, cellulose synthesis, cytokinesis, and cell expansion. J. Exp. Bot. **59:** 361–376.

Curtis, M.D., and Grossniklaus, U. (2003). A Gateway cloning vector set for high-throughput functional hnalysis of henes in planta. Plant Physiol. **133:** 462–469.

Dhonukshe, P., Aniento, F., Hwang, I., Robinson, D.G., Mravec, J., Stierhof, Y.D., and Friml, J. (2007). Clathrin-mediated constitutive endocytosis of PIN auxin efflux carriers in *Arabidopsis.* Curr. Biol. **17:** 520–527.

Ding, J., Segarra, V.A., Chen, S., Cai, H., Lemmon, S.K., and Ferro-Novick, S. (2015). Auxilin facilitates membrane traffic in the early secretory pathway. Mol. Biol. Cell **27:** 1–36.

Di Rubbo, S., et al. (2013). The clathrin adaptor complex AP-2 mediates endocytosis of BRASSINOSTEROID INSENSITIVE1 in *Arabidopsis.* Plant Cell **25:** 2986–2997.

Emons, A.M.C., and Traas, J.A. (1986). Coated pits and coated vesicles on the plasma membrane of plant cells. Eur. J. Cell Biol. **41:** 57–64.

Fan, L., Hao, H., Xue, Y., Zhang, L., Song, K., Ding, Z., and Botella, M.A., Wang, H., Lin, J. (2013). Dynamic analysis of *Arabidopsis* AP2 σ subunit reveals a key role in clathrin-mediated endocytosis and plant development. Development **140:** 3826–3837.

Feraru, E., Paciorek, T., Feraru, M.I., Zwiewka, M., De Groodt, R., De Rycke, R., Kleine-Vehn, J., and Friml, J. (2010). The AP-3 β-adaptin mediates the biogenesis and function of lytic vacuoles in *Arabidopsis.* Plant Cell **22:** 2812–2824.

Friml, J., et al. (2004). A PINOID-dependent binary switch in apical-basal PIN polar targeting directs auxin efflux. Science **306:** 862–865.

Fuji, K., Shirakawa, M., Shimono, Y., Kunieda, T., Fukao, Y., Koumoto, Y., Takahashi, H., Hara-Nishimura, I., and Shimada, T. (2016). The adaptor complex AP-4 regulates vacuolar protein sorting at the trans-Golgi network by interacting with VACUOLAR SORTING RECEPTOR1. Plant Physiol. **170:** 211–219.

Gadeyne, A., et al. (2014). The TPLATE adaptor complex drives clathrin-mediated endocytosis in plants. Cell **156:** 691–704.

Galway, M.E., Rennie, P.J., and Fowke, L.C. (1993). Ultrastructure of the endocytotic pathway in glutaraldehyde-fixed and high-pressure frozen/freeze-substituted protoplasts of white spruce (*Picea glauca*). J. Cell Sci. **3:** 847–858.

Gao, B., Biosca, J., Craig, E.A., Greene, L.E., and Eisenberg, E. (1991). Uncoating of coated vesicles by yeast hsp70 proteins. J. Biol. Chem. **266:** 19565–19571.

Greener, T., Grant, B., Zhang, Y., Wu, X., Greene, L.E., Hirsh, D., and Eisenberg, E. (2001). *Caenorhabditis elegans* auxilin: a J-domain protein essential for clathrin-mediated endocytosis in vivo. Nat. Cell Biol. **3:** 215–219.

Henne, W.M., Boucrot, E., Meinecke, M., Evergren, E., Vallis, Y., Mittal, R., and McMahon, H.T. (2010). FCHo proteins are nucleators of clathrin-mediated endocytosis. Science **328:** 1281–1284.

Irani, N.G., et al. (2012). Fluorescent castasterone reveals BRI1 signaling from the plasma membrane. Nat. Chem. Biol. **8:** 583–589.

Ischebeck, T., et al. (2013). Phosphatidylinositol 4,5-bisphosphate influences PIN polarization by controlling clathrin-mediated membrane trafficking in *Arabidopsis.* Plant Cell **25:** 4894–4911.

Jelínková, A., Malínská, K., Simon, S., Kleine-Vehn, J., Pařezová, M., Pejchar, P., Kubeš, M., Martinec, J., Friml, J., Zažímalová, E., and Petrášek, J. (2010). Probing plant membranes with FM dyes: tracking, dragging or blocking? Plant J. **61:** 883–892.

Kang, B.H., Busse, J.S., Dickey, C., Rancour, D.M., and Bednarek, S.Y. (2001). The *Arabidopsis* cell plate-associated dynamin-like protein, ADL1Ap, is required for multiple stages of plant growth and development. Plant Physiol. **126:** 47–68.

Kang, B.H., Rancour, D.M., and Bednarek, S.Y. (2003). The dynamin-like protein ADL1C is essential for plasma membrane maintenance during pollen maturation. Plant J. **35:** 1–15.

Karimi, M., Inzé, D., and Depicker, A. (2002). GATEWAY™ vectors for Agrobacterium-mediated plant transformation. Trends Plant Sci. **7:** 193–195.

Kerppola, T.K. (2009). Visualization of molecular interactions using analysis: Characteristics of protein fragment complementation. Chem. Soc. Rev. **38:** 2876–2886.

Kim, S.Y., Xu, Z.-Y., Song, K., Kim, D.H., Kang, H., Reichardt, I., Sohn, E.J., Friml, J., Juergens, G., and Hwang, I. (2013). Adaptor protein complex 2-mediated endocytosis Is crucial for male reproductive organ development in *Arabidopsis.* Plant Cell **25:** 2970–2985.

Kitakura, S., Vanneste, S., Robert, S., Löfke, C., Teichmann, T., Tanaka, H., and Friml, J. (2011). Clathrin mediates endocytosis and polar distribution of PIN auxin transporters in *Arabidopsis.* Plant Cell **23:** 1920–1931.

Kolb, C., Nagel, M.-K., Kalinowska, K., Hagmann, J., Ichikawa, M., Anzenberger, F., Alkofer, A., Sato, M.H., Braun, P., and Isono, E. (2015). FYVE1 is essential for vacuole biogenesis and intracellular trafficking in *Arabidopsis.* Plant Physiol. **167:** 1361–1373.

Konopka, C.A., Backues, S.K., and Bednarek, S.Y. (2008). Dynamics of *Arabidopsis* dynamin-related protein 1C and a clathrin light chain at the plasma membrane. Plant Cell **20:** 1363–1380.

Konopka, C.A., and Bednarek, S.Y. (2008). Variable-angle epifluorescence microscopy: A new way to look at protein dynamics in the plant cell cortex. Plant J. **53:** 186–196.

Lam, B.C., Sage, T.L., Bianchi, F., and Blumwald, E. (2001). Role of SH3 domain-containing proteins in clathrin-mediated vesicle trafficking in *Arabidopsis.* Plant Cell **13:** 2499–2512.

Lauber, M.H., Waizenegger, I., Steinmann, T., Schwarz, H., Mayer, U., Hwang, I., Lukowitz, W., and Jürgens, G. (1997). KNOLLE protein is a cytokinesis-specific syntaxin. Cell **139:** 1485–1493.

Lee, D.-W., Wu, X., Eisenberg, E., and Greene, L.E. (2006). Recruitment dynamics of GAK and auxilin to clathrin-coated pits during endocytosis. J. Cell Sci. **119:** 3502–3512.

Lee, D., Zhao, X., Yim, Y.-I., Eisenberg, E., and Greene, L.E. (2008). Essential role of cyclin-G–associated kinase (auxilin-2) in developing and mature mice. Mol. Biol. Cell **19:** 2766–2776.

Van Leene, J., et al. (2014). An improved toolbox to unravel the plant cellular machinery by tandem affinity purification of *Arabidopsis* protein complexes. Nat. Protoc. **10:** 169–187.

Livak, K.J., and Schmittgen, T.D. (2001). Analysis of relative gene expression data using real-time quantitative PCR and the $2-\Delta\Delta CT$ method. Methods **25:** 402–408.

Łangowski, Ł., Wabnik, K., Li, H., Vanneste, S., Naramoto, S., Tanaka, H., and Friml, J. (2016). Cellular mechanisms for cargo delivery and polarity maintenance at different polar domains in plant cells. Cell Discov. **2:** 16018.

Massol, R.H., Boll, W., Griffin, A.M., and Kirchhausen, T. (2006). A burst of auxilin recruitment determines the onset of clathrin-coated vesicle uncoating. Proc. Natl. Acad. Sci. USA **103:** 10265–10270.

McMahon, H.T., and Boucrot, E. (2011). Molecular mechanism and physiological functions of clathrin-mediated endocytosis. Nat. Rev. Mol. Cell Biol. **12:** 517–533.

Mersey, B.G., Griffing, L.R., Rennie, P.J., Fowke, L.C., Mersey, B.G., Griffing, L.R., Rennie, P.J., and Fowke, L.C. (1985). The isolation of coated vesicles from protoplasts of soybean. Planta **163:** 317–327.

Mravec, J., et al. (2009). Subcellular homeostasis of phytohormone auxin is mediated by the ER-localized PIN5 transporter. Nature **459:** 1136–1140.

Nagel, M.-K., Kalinowska, K., Vogel, K., Reynolds, G.D., Wu, Z., Anzenberger, F., Ichikawa, M., Tsutsumi, C., Sato, M.H., Kuster, B., Bednarek, S.Y., and Isono, E. (2017). *Arabidopsis* SH3P2 is an ubiquitin-binding protein that functions together with ESCRT-I and the deubiquitylating enzyme AMSH3. Proc. Natl. Acad. Sci. USA **114:** E7197–E7204.

Naramoto, S., Otegui, M.S., Kutsuna, N., de Rycke, R., Dainobu, T., Karampelias, M., Fujimoto, M., Feraru, E., Miki, D., Fukuda, H., Nakano, A., and Friml, J. (2014). Insights into the localization and function of the membrane trafficking regulator GNOM ARF-GEF at the Golgi apparatus in *Arabidopsis.* Plant Cell **26:** 3062–3076.

Nodzyński, T., Vanneste, S., Zwiewka, M., Pernisová, M., Hejátko, J., and Friml, J. (2016). Enquiry into the topology of plasma membrane-localized PIN auxin transport components. Mol. Plant **9:** 1504–1519.

Ortiz-Morea, F.A., et al. (2016). Danger-associated peptide signaling in *Arabidopsis* requires clathrin. Proc. Natl. Acad. Sci. USA **113:** 11028–11033.

Paciorek, T., Zazímalová, E., Ruthardt, N., Petrásek, J., Stierhof, Y.D., Kleine-Vehn, J., Morris, D.A., Emans, N., Jürgens, G., Geldner, N., and Friml, J. (2005). Auxin inhibits endocytosis and promotes its own efflux from cells. Nature **435:** 1251–1256.

Park, M., Song, K., Reichardt, I., Kim, H., Mayer, U., Stierhof, Y.-D., Hwang, I., and Jurgens, G. (2013). *Arabidopsis* mu-adaptin subunit AP1M of adaptor protein complex 1 mediates late secretory and vacuolar traffic and is required for growth. Proc. Natl. Acad. Sci. USA **110:** 10318–10323.

Renard, H.-F., et al. (2014). Endophilin-A2 functions in membrane scission in clathrin-independent endocytosis. Nature **517:** 493–496.

Richter, J., Watson, J.M., Stasnik, P., Borowska, M., Neuhold, J., Stolt-Bergner, P., Schoft, V.K., and Hauser, M.T. (2018). Multiplex mutagenesis with CRISPR/CAS9 exposes growth regulatory roles of four clustered CrRLK1L to metal ions. submitted.

Richter, S., Kientz, M., Brumm, S., Nielsen, M.E., Park, M., Gavidia, R., Krause, C., Voss, U., Beckmann, H., Mayer, U., Stierhof, Y.D., and Jürgens, G. (2014). Delivery of endocytosed proteins to the cell-division plane requires change of pathway from recycling to secretion. eLife **2014:** 1–16.

Robinson, D.G., and Pimpl, P. (2014). Clathrin and post-Golgi trafficking: A very complicated issue. Trends Plant Sci. **19:** 134–139.

Salanenka, Y., Verstraeten, I., Löfke, Ch., Tabata, K., Naramoto, S., Glanc, M., and Friml, J. (2018). Gibberellin DELLA signaling targets the retromer complex to redirect protein trafficking to the plasma membrane. Proc. Natl. Acad. Sci. USA **pii:** 201721760.

Sauer, M., Paciorek, T., Benková, E., and Friml, J. (2006). Immunocytochemical techniques for whole-mount *in situ* protein localization in plants. Nat. Protoc. **1:** 98–103.

Scheuring, D., Viotti, C., Kruger, F., Kunzl, F., Sturm, S., Bubeck, J., Hillmer, S., Frigerio, L., Robinson, D.G., Pimpl, P., and Schumacher, K. (2011). Multivesicular bodies mature from the trans-Golgi network/early endosome in *Arabidopsis.* Plant Cell **23:** 3463–3481.

Song, K., Jang, M., Kim, S.Y., Lee, G., Lee, G.-J., Kim, D.H., Lee, Y., Cho, W., and Hwang, I. (2012). An A/ENTH domain-containing protein functions as an adaptor for clathrin-coated vesicles on the growing cell plate in *Arabidopsis* root cells. Plant Physiol. **159:** 1013–1025.

Suetsugu, N., Kagawa, T., Wada, M., and Corporation, T. (2005). An auxilin-like J-domain protein, JAC1, regulates phototropin-mediated chloroplast movement. Plant Physiol. **139:** 151–162.

Tanaka, H., Kitakura, S., Rakusová, H., Uemura, T., Feraru, M.I., de Rycke, R., Robert, S., Kakimoto, T., and Friml, J. (2013). Cell polarity and patterning by PIN trafficking through early endosomal compartments in *Arabidopsis thaliana.* PLoS Genet. **9:** 1–9.

Tanchak, M.A., Griffing, L.R., Mersey, B.G., and Fowke, L.C. (1984). Endocytosis of cationized ferritin by coated vesicles of soybean protoplasts. Planta **162:** 481–486.

Tejos, R., Sauer, M., Vanneste, S., Palacios-Gomez, M., Li, H., Heilmann, M., van Wijk, R., Vermeer, J.E.M., Heilmann, I., Munnik, T., and Friml, J. (2014). Bipolar plasma membrane distribution of phosphoinositides and their requirement for auxin-mediated cell polarity and patterning in *Arabidopsis.* Plant Cell **26:** 2114–2128.

Ungewickell, E., Ungewickell, H., Holstein, S.E.H., Linder, R., Prasad, K., Barouch, W., Martin, B., Greene, L.E., and Eisenberg, E. (1995). Role of auxilin in uncoating clathrin-coated vesicles. Nature **378:** 632–635.

von Wangenheim, D., Hauschild, R., Fendrych, M., Barone, V., Benková, E., and Friml, J. (2017). Live tracking of moving samples in confocal microscopy for vertically grown roots. eLife **6:** 1–20.

Wang, C., Yan, X., Chen, Q., Jiang, N., Fu, W., Ma, B., Liu, J., Li, C., Bednarek, S.Y., and Pan, J. (2013a). Clathrin light chains regulate clathrin-mediated trafficking, auxin signaling, and development in *Arabidopsis.* Plant Cell **25:** 499–516.

Wang, J.-G., Li, S., Zhao, X.-Y., Zhou, L.-Z., Huang, G.-Q., Feng, C., and Zhang, Y. (2013b). HAPLESS13, the *Arabidopsis* μ1 adaptin, is essential for protein sorting at the trans-Golgi network/early endosome. Plant Physiol. **162:** 1897–1910.

Wang, X., Cai, Y., Wang, H., Zeng, Y., Zhuang, X., Li, B., and Jiang, L. (2014). Trans-Golgi network-located AP1 gamma adaptins mediate dileucine motif-directed vacuolar targeting in *Arabidopsis.* Plant Cell **26:** 4102–4118.

Widhalm, J.R., Ducluzeau, A.L., Buller, N.E., Elowsky, C.G., Olsen, L.J., and Basset, G.J.C. (2012). Phylloquinone (vitamin K1) biosynthesis in plants: Two peroxisomal thioesterases of lactobacillales origin hydrolyze 1,4-dihydroxy-2-naphthoyl-coa. Plant J. **71:** 205–215.

Xing, Y., Böcking, T., Wolf, M., Grigorieff, N., Kirchhausen, T., and Harrison, S.C. (2010). Structure of clathrin coat with bound Hsc70 and auxilin: mechanism of Hsc70-facilitated disassembly. EMBO J. **29:** 655–665.

Yamaoka, S., Shimono, Y., Shirakawa, M., Fukao, Y., Kawase, T., Hatsugai, N., Tamura, K., Shimada, T., and Hara-Nishimura, I. (2013). Identification and dynamics of *Arabidopsis* Adaptor Protein-2 complex and its involvement in floral organ development. Plant Cell **25:** 2958–2969.

Yim, Y.-I., Sun, T., Wu, L.-G., Raimondi, A., De Camilli, P., Eisenberg, E., and Greene, L.E. (2010). Endocytosis and clathrin-uncoating defects at synapses of auxilin knockout mice. Proc. Natl. Acad. Sci. USA **107:** 4412–4417.

Yoshinari, A., Fujimoto, M., Ueda, T., Inada, N., Naito, S., and Takano, J. (2016). DRP1-dependent endocytosis is essential for polar localization and boron-induced degradation of the borate transporter BOR1 in *Arabidopsis thaliana.* Plant Cell Physiol. **57:** 1985–2000.

Zhang, Y., Persson, S., Hirst, J., Robinson, M.S., van Damme, D., and Sánchez-Rodríguez, C. (2015). Change your Tplate, change your fate: Plant CME and beyond. Trends Plant Sci. **20:** 41–48.

Zhao, X., Greener, T., Al-Hasani, H., Cushman, S.W., Eisenberg, E., and Greene, L.E. (2001). Expression of auxilin or AP180 inhibits endocytosis by mislocalizing clathrin: evidence for formation of nascent pits containing AP1 or AP2 but not clathrin. J. Cell Sci. **114:** 353–365.

Zhuang, X., Cui, Y., Gao, C., and Jiang, L. (2015). Endocytic and autophagic pathways crosstalk in plants. Curr. Opin. Plant Biol. **28:** 39–47.

Zhuang, X., Wang, H., Lam, S.K., Gao, C., Wang, X., Cai, Y., and Jiang, L. (2013). A BAR-domain protein SH3P2, which binds to phosphatidylinositol 3-phosphate and ATG8, regulates autophagosome formation in *Arabidopsis.* Plant Cell **25:** 4596–4615.

Zouhar, J., and Sauer, M. (2014). Helping hands for budding prospects: ENTH/ANTH/VHS accessory proteins in endocytosis, vacuolar transport, and secretion. Plant Cell **26:** 1–13.

Zwiewka, M., Feraru, E., Möller, B., Hwang, I., Feraru, M.I., Kleine-Vehn, J., Weijers, D., and Friml, J. (2011). The AP-3 adaptor complex is required for vacuolar function in *Arabidopsis.* Cell Res. **21:** 1711–1722.